

1 **Drainage network evolution and reconstruction in an open pit** 2 **kaolin mine at the edge of the Alto Tajo Natural Park**

3 Ignacio Zapico^{a,b*}, Jonathan B. Laronne^c, Lázaro Sánchez Castillo^d, José F. Martín
4 Duque^{a,b}

5

6 ^a Geodynamics, Stratigraphy and Paleontology Department, Complutense University,
7 28040 Madrid, Spain

8 ^b Instituto de Geociencias, IGEO (CSIC, UCM), 28040 Madrid, Spain

9 ^c Department of Geography and Environmental Development, Ben-Gurion University of
10 the Negev, P.O. Box 653, Beer-Sheva 84105, Israel

11 ^d Department of Mining and Geologic Engineering, Polytechnic University of Madrid,
12 Madrid 28003, Spain

13

14 *Corresponding author: e-mail: izapico@ucm.es

15 **Highlights**

- 16 • A mine dismantled and obliterated an existing drainage network
- 17 • The spontaneous re-development of such drainage network is risking a natural
18 park
- 19 • We propose mine rehabilitation reconstructing functional drainage basins and
20 networks
- 21 • Fluvial geomorphology provides scientific basis for functional mine rehabilitation

22 **Abbreviations:** DEM - Digital Elevation Models; DoD - DEMs of Difference; SfM -
23 Structure from Motion; UAV - Unmanned Aerial Vehicle; LiDAR - Light Detection and
24 Ranging; GCD - Geomorphic Change Detection; ALS - Aerial Laser Scanning; HRT -
25 High Resolution Topography

26 **Abstract:** Landform instability of the abandoned Nuria kaolin mine, surrounding the Alto
27 Tajo Natural Park in Spain, has caused frequent and severe environmental impacts due
28 to deficient mining practices, environmental mismanagement and closure planning.
29 Geomorphic instability has caused widespread soil erosion and elevated sediment yields
30 with off-site effects. We quantified such land instability, the evolution of the resulting
31 drainage networks and catchments, and ensuing gully processes. High Resolution
32 Topography sources were compared with historic maps and photos. The current mine
33 rehabilitation practices are depicted based on a geomorphic approach that introduces a
34 sustainable drainage system designed to avoid detected risks. Our aim is reconstructing
35 fluvial channels and related hillslopes that mimic their natural counterparts adapted to a
36 rehabilitation of pre-existing gradient terraces. We demonstrate that: i) mining activity
37 produced a 31-58% decrease in the original site drainage network ii) a post-mining active
38 advancing gully is an indicator of drainage network redevelopment advancing toward an
39 upstream pond with flash-flooding risk ; iii) a geomorphic designed and constructed
40 fluvial network and proper drainage density adapted to pre-existing gradient-terraces
41 seeks reestablishing stability; and iv) in absence of sufficient funding for rehabilitation,
42 public/private collaboration agreements play an important role to reinstate landscape
43 stability of abandoned or erroneously restored mines.

44 **Keywords:** erosion, drainage network, geomorphic rehabilitation, mine waste
45 stabilization, Alto Tajo Natural Park, topography, geomorphic change detection

46 **1. Introduction**

47 Mining is essential for human activities. Nevertheless, it is responsible for many
48 environmental impacts due to the processes of extraction and processing. It disturbs not
49 only the land where it is developed, through the loss of landforms, soil, vegetation and
50 fauna, but also impacts the downstream landscape with its polluted spillages (Mossa and
51 James, 2013; Tarolli et al., 2018). Increase in stormwater runoff and sediment yield from

52 mining areas has been widely documented (Katpatal et al., 2017). Several environmental
53 land management control measures apply to mine operations and can often be achieved
54 in parallel to modern mining activities. However, a major challenge arises at the end of
55 mining operations, when a closure plan to permanently stabilize and rehabilitate the
56 mined area, including its facilities, is enforced. At this stage, owners are required to
57 minimize possible future land degradation and social impacts. Actions of post-mining
58 environmental mitigation are expensive and can delay the release of the mining bond.
59 Closure plans integrated with mining operations provide best stability and environmental
60 results at the cheapest cost (Hannan, 1984). In many cases, by lacking this integration,
61 the unsuccessful rehabilitation areas cause severe environmental impacts (Reed and
62 Kite, 2020).

63 Stability issues causing damages and pollution in rehabilitated areas often occur due to
64 erosion vulnerability of traditional straight shapes of the constructed landforms, and
65 because the rigid erosion control structures are unable to manage runoff in the long term,
66 thereby generating erosion of hillslopes and ditches (Sawatsky and Beersing, 2014). For
67 instance, in a rehabilitation study of three West Virginian mines, a drainage network that
68 did not reproduce natural analogues in terms of density and bankfull geometry was the
69 main factor causing severe gully erosion and landslides (Kite et al., 2004). Whereas that
70 multi-temporal study utilized topographic maps and conventional GPS, the number,
71 length of gullies and landslide frequency were recently examined in reclaimed central
72 Appalachia using Light Detection and Ranging (LiDAR) data from a single date (Reed
73 and Kite, 2020). They also interpreted how these erosion shapes appeared due to faulty
74 rehabilitation practices, such as retention cells in the upper part of the terraces. These
75 valuable studies draw attention to damages incurred due to lack of shaping a proper
76 drainage network. However, long-term studies combining both multi-temporal analyses
77 and accurate topographic data are required to improve quantification of erosional stability
78 (Reed and Kite, 2020).

79 Recovering long-term terrain stability extends thinking beyond structures such as
80 ditches, dumps and ponds, to designing and constructing functional landscapes with
81 streams, hillslopes or wetlands that function independently based on hydrologic
82 conditions (McKenna and Dawson, 1997). Such features have to be organized as self-
83 regulating erosional catchments (Stiller et al., 1980). In this context, Fluvial Geomorphic
84 Rehabilitation based on a surficial drainage management (Bugosh and Epp, 2019), with
85 specific methods such as GeoFluv-Natural Regrade (Bugosh and Epp, 2019; Zapico et
86 al., 2018), is a proliferating rehabilitation technique to achieve long-term erosion stability
87 of land disturbed by mining. This methodology has been catalogued as a Best Available
88 Technique for the management of waste from extractive industries in accordance with
89 the European Directive 2006/21/EC (Martin Duque et al., 2019). It can also be used in
90 combination with Landscape Evolution Models such as SIBERIA, to evaluate the stability
91 of designs and successively improve them (Hancock et al., 2019). Several fluvial
92 geomorphic mine-rehabilitation examples exist in the United States (Bugosh and Epp,
93 2019) and Spain (Zapico et al., 2018). In those cases, this approach reinstated functional
94 landscapes, which correspond site erosion values to those of the surrounding natural
95 landscapes (baseline), inclusive of successful stabilization of a landslide (Zapico et al.,
96 2020). This accomplishment derives from the introduction of a drainage density similar
97 to natural reference landscapes and designing as well as constructing fluvial channels
98 with similar longitudinal and cross-sectional shapes as the natural ones. Indeed, such
99 criteria are required in credible landscape engineering (McKenna and Dawson, 1997).

100 Today, worldwide mine rehabilitation is still dominated by a focus on soil and vegetation
101 management. In most countries, this focus is fostered by regulations, seeking that mine
102 rehabilitation require “safe, stable, non-polluting post-mining landforms”, as in Australia
103 (Howard et al., 2011). However, a growing body of literature (e.g.; McKenna and
104 Dawson, 1997; or Kite et al., 2004) has demonstrated that, without a proper
105 consideration of natural drainage systems in mine rehabilitation, instability occurs. The

106 United States Surface Mining Control and Reclamation Act (SMCRA, 1977) was the
107 pioneering law regarding mine rehabilitation, demanding that the extent to which surface
108 configuration achieved by backfilling and grading of a mined area must closely resemble
109 the general surface configuration of the land prior to mining, and should blend into, and
110 complement the drainage pattern of the surrounding terrain. It is surprising how, 44 years
111 later, it is still the only mine rehabilitation law, worldwide, with such focus. Thus, although
112 the example we provide is site-specific, it shows a contribution with global implications,
113 at the least for fluvial processes, acting on the overwhelming majority of the ice-free land
114 surface.

115 Detailed topographic monitoring is required to understand and manage drastic
116 landscape modifications due to mining and rehabilitation practices (Ross et al., 2016).
117 Some of these evaluations are undertaken by comparison of topographies. In earth
118 science, the most common methodology to quantify topographic change is Geomorphic
119 Change Detection (GCD) through Digital Elevation Models (DEMs) of Difference (DoDs);
120 its use in mining projects is increasing (Xiang et al., 2018; Zapico et al., 2018).
121 Traditionally, topographic surveys are undertaken with differential GPS (dGPS), Total
122 Station, Terrestrial Laser Scanning or Aerial Laser Scanning (ALS). However, an
123 emerging technique, Structure from Motion (SfM) combined with Unmanned Aerial
124 Vehicles (UAVs), SfM-UAV, is replacing these technologies due to its ease of use, lower
125 cost and high accuracy and resolution (Carrivick et al., 2016). In mining areas SfM-UAV
126 is used to study mining stability (López-Vinielles et al., 2020) and to monitor mining
127 activity (Carabassa et al., 2020). Historically, most mining areas were sanctioned, such
128 that early site data based on modern topographic techniques are typically unavailable.
129 In those cases, studies can be completed with historic topographic maps (Zapico et al.,
130 2020).

131 The primary Spanish kaolin extraction is undertaken in an area surrounding one of the
132 most biodiverse natural parks in Spain, the Alto Tajo. Here, abandoned mines cause

133 severe impacts on the natural fluvial system. They experience risky landslides and
134 produce high sediment yields (Zapico et al., 2017), arising due to their unstable
135 landforms and lack of erosive-sedimentary control measures (Martín-Moreno et al.,
136 2018). The Nuria mine is one such abandoned operation. It was closed because
137 extension of a new concession was rejected, due to faulty environmental performance
138 and an inadequate closure plan. Therefore, the bond release was not returned to the
139 owners. This guarantee was used to stabilize a rotational landslide in a waste dump
140 using geomorphic rehabilitation (Zapico et al., 2020). Other unstable areas continue
141 posing risks, and several monitoring, analysis and stability measures are being
142 accomplished through agreements of public and private collaboration. Using High
143 Resolution Topographies (HRTs), a historic topographic map and photos, the evolution
144 of an existing drainage network, its catchments and a gully were studied. Fluvial
145 Geomorphic Rehabilitation is proposed as a technique to stabilize the detected
146 instabilities in the Nuria mine. Our aims are to: i) qualify and quantify the temporal change
147 in drainage network density and catchment changes due to mining activity and
148 rehabilitation practices; ii) quantify the main current erosive gully processes threatening
149 mine stability; iii) describe the versatile application of a geomorphic rehabilitation to an
150 unstable waste dump requiring innovative adaptation to preexistent-terraces; and iv)
151 discuss the importance of public-private collaboration to solve environmental problems
152 in abandoned or deficiently restored mines.

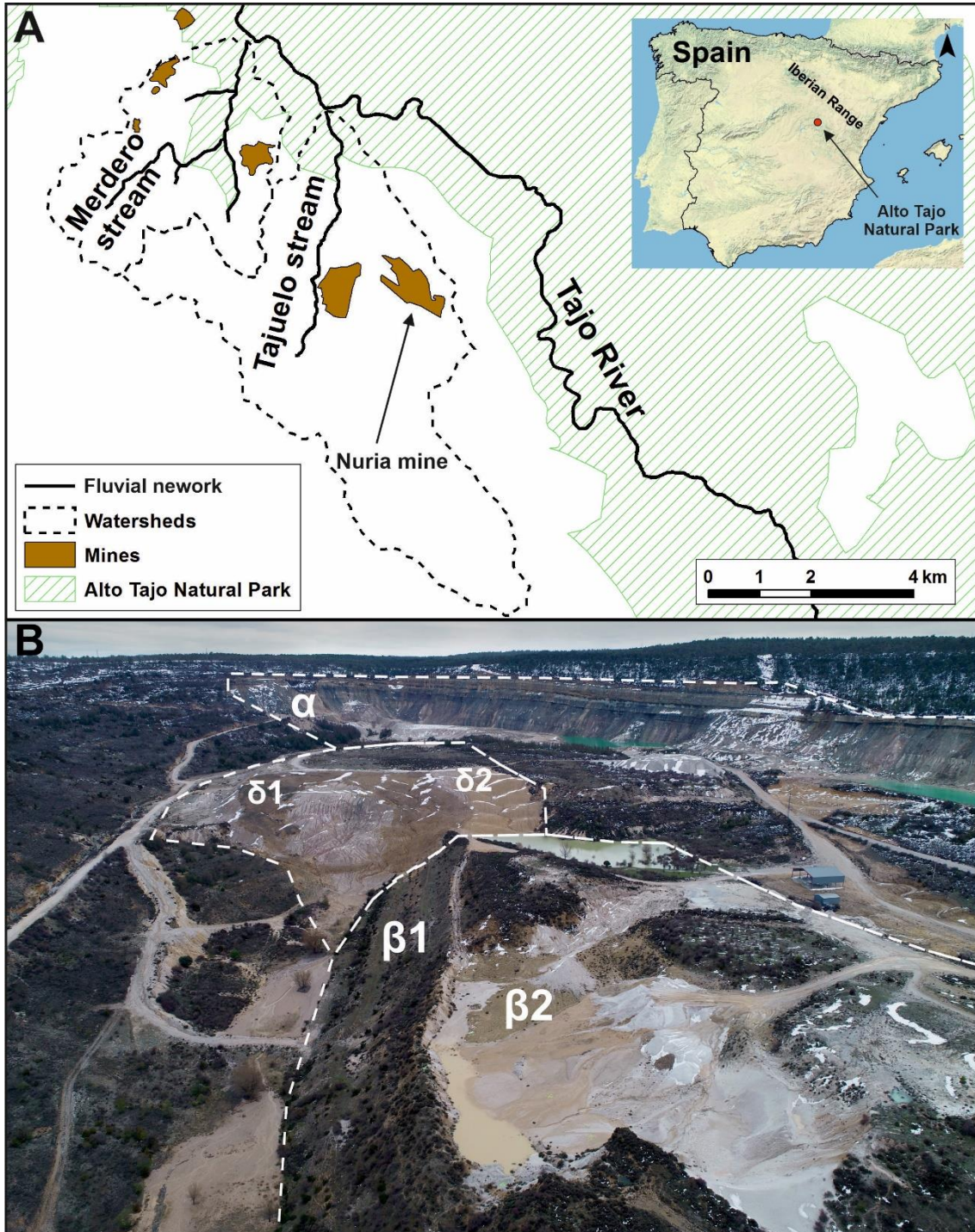
153 **2. Material and methods**

154 *2.1. Study area*

155 2.1.1. The Alto Tajo Natural Park

156 The Alto Tajo Natural Park is a well-known Spanish protected area formed by a dense
157 network of fluvial canyons with steep and long slopes geologically incised by the Tajo
158 River and its tributaries. The main feature is the high-quality water of its fluvial system

159 and the ecosystems that it supports. The best national kaolin has been extracted during
160 the last decades at four mines surrounding the park (Fig. 1). The Nuria and the Santa
161 Engracia mines are now abandoned; sediment yield from these mines is considered by
162 the natural park managers as the main environmental risk to the Alto Tajo Natural Park.
163 The lack of proper erosion control measures leads not only to adverse on-site impacts,
164 but also to off-site effects. Two other active mines, the Machorro and the María José, are
165 well-known for applying remedies: maintained sedimentation ponds (Zapico et al., 2021)
166 and geomorphic rehabilitation (Garbarino et al., 2018).



168

169

170

171

172

173

174

175

Figure 1. Location of the Alto Tajo Natural Park and the Nuria mine (A), and oblique view of the Nuria mine on 15.04.2018 (B). Redrawn from Zapico et al. (2018). The mine is classified into three areas: “ α ” an open pit with three ponds near the highwall base; “ β ” an altered terraced waste dump to reprocess its wastes (“ $\beta 1$ ” part of the terraces not modified and “ $\beta 2$ ” part of the terraces removed); and “ δ ” a terraced waste dump that experienced a landslide and severe erosion, thereafter stabilized (“ $\delta 1$ ”) and restored (“ $\delta 2$ ”) with geomorphic rehabilitation. Photos by DGDRONE (2018).

176 2.1.2 History of the Nuria mine

177 The Nuria mine occupies an oval-shaped structural valley, with the pointed side facing
178 the southeast. The valley is open towards the northwest by the erosion of two main
179 drainage lines: the Matalascabras stream and the Carrascalejo creek, both sub-
180 catchments of the Tajuelo stream, a tributary of the Tajo River (Fig. 1). The valley sides
181 are formed by typical scarps of the mesas, cuestras and hogbacks that surround the
182 valley. The bottom valley is excavated in Jurassic limestones and Cretaceous sands,
183 silts and clays (Weald facies); the valley walls are shaped in silica and kaolinite sands
184 (Utrillas facies). The Carrascalejo creek lacks a proper fluvial headwater, which is cut by
185 the Matalascabras valley. This is clear evidence of an ancient stream capture, in which
186 the upstream erosion of the Matalascabras catchment captured the Carrascalejo
187 headwaters.

188 Mining operations started here approximately in 1982 and initially the mine was
189 adequately rehabilitated. This resulted in a series of terraces, built as progressive
190 rehabilitation (“β” zone in Fig. 1) over 30 years, that have been mostly stable, and are
191 now successfully colonized by vegetation. However, a change of owner brought
192 cessation to mine rehabilitation. Furthermore, some restored areas were either buried
193 with new waste dumps or modified. Due to incorrect environmental performance and an
194 inadequate closure plan, a new concession extension was rejected, and the bond
195 release was not returned to the owners. The ‘final’ scenario of the Nuria mine, when
196 extractive activity was ended by the regulators in 2010, was a very heterogeneous site,
197 with rehabilitated areas coexisting with large tracts lacking measurements of recovery.
198 Hence, mass movements and gullying have progressed, generating risky situations,
199 such as active landslides and potential flash flooding. The situation at the end of the
200 activity was as follows (Fig. 1):

201 - “α” zone. The open pit and three ponds located at the highwall base were left without
202 rehabilitation measures or proper drainage systems. Two of the ponds were excavated

203 on original ground and the third, located most upstream, was formed with an earth dam
204 of unconsolidated and sorted sand. This is causing two main risks: i) gully and ravine
205 erosion processes are redeveloping the drainage network, advancing towards a series
206 of ponds located at the highwall foot; and, ii) three ponds are accumulating a large
207 amount of water, so the hazard of dam failure or spilling if captured by gully headcutting
208 has a potential risk to cause harmful flash floods.

209 - “β” zone. These are the oldest terraces constructed in the first stages of the mine by
210 the original owners. In the absence of significant erosion, vegetation has grown (“β1”),
211 to successful rehabilitation, with some uncertainty about long-term stability. However,
212 parts of the highest terraces were modified by the last owner to reprocess waste material
213 “β2”. At the end of this activity, the waste material was left at the top of the terraces, has
214 been exposed to erosion and is threatening the stability of the entire rehabilitation.

215 - “δ” zone. A waste dump restored by gradient terraces constructed over part of the
216 terraces in “β” zone and over the center of a valley, obstructed drainage in the natural
217 ephemeral channel. It experienced a large rotational landslide (“δ1”) and severe erosion
218 (“δ2”). During 2014-17 these were stabilized and rehabilitated (Zapico et al., 2020).

219 *2.2. Topographic sources and analyses*

220 Four types of topographic sources were used (Table 1): i) a 1:25,000 topographic map
221 with 10 m equidistant contours (IGN, 1995); ii) two high resolution LiDAR point clouds
222 covering the entire mine were surveyed by ALS and provided by the Spanish National
223 Plan for Aerial Orthophotography (PNOA, 2018, 2009); iii) a drone paired with an SfM
224 image processing (SfM-UAV) survey for the “β” zone; iv) a point cloud surveyed with a
225 Leica 1200 dGPS. The SfM-Survey was performed in 2018 with 487 photographs taken
226 at zenithal and oblique angles by a DJI Phantom 4 Pro drone kept at a constant altitude
227 with a maximum height of 120 m above ground. The Ground Sample Distance (GSD)
228 was 3.09 cm pix⁻¹ and the final pixel error was 0.2. Altogether 30 targets were placed as

229 check (11) or control points (19). The targets were measured with the dGPS.
 230 Photographs and control points were processed with Agisoft PhotoScan software. The
 231 main parameters used in this software were: alignment accuracy, Highest; key point limit,
 232 40,000; Tie point limit, 4,000; dense point cloud quality, High; Filter mode, Aggressive.
 233 Vegetation was `cleaned` and check points were used to measure the accuracy using
 234 the LP360 Advanced edition software (Qcoherent, 2018).

235 Table 1. Topographic data availability and related accuracy.

date	source/method	photos #	point cloud density pts m ⁻²	RMSE check points		
				n° #	x,y m	z
1984 ¹	25,000 topographic map with 10 m equidistant contour	n.d.	n.d.	n.d.	n.d.	1.93 ²
02.02.2010	LiDAR-ALS	n.d.	0.5	n.d.	0.3 ³	0.2 ³
29.06.2018		n.d.	1	n.d.	0.3 ³	0.2 ³
15.04.2018	SfM-UAV	487	373	11	0.14	0.04
17.04.2020	dGPS	n.d.	0.09	n.d.	0.03 ⁴	0.03 ⁴

236 n.d. - no data.

237 ¹ This map was published in 1995 and prepared with photogrammetric data dated 1984;

238 ² Derived from a direct comparison with 2009 topographic data of those areas without
 239 topographic changes between the two dates;

240 ³ technical specification (PNOA, 2018, 2009);

241 ⁴ local accuracy was not measured for the points surveyed with the DGPS. We adopt values
 242 reported elsewhere using a similar instrument (Cucchiario et al., 2018; Lucieer et al., 2014).

243
 244 The topographic map and the two LiDAR-ALS data were used to delineate catchments
 245 and the drainage networks before and after the Nuria mine appearance by using an
 246 automatic catchment and stream delineation procedure in ArcGIS Pro 2.5.1 (ESRI,
 247 2020). These drainage networks were also reviewed and corrected as needed, using the
 248 more recent public orthophotos for each topographic source and photo interpretation.
 249 Drainage network lengths were associated with the mining catchment area to define the
 250 temporal evolution of drainage density evolution. Channels of each drainage network
 251 were classified into four types: i) original, before mining activity; ii) unpaved road ditches

252 built by the mining operators; iii) gullies developed due to fluvial erosion; iv) drainage
253 systems equivalent to natural ones introduced by Fluvial Geomorphic Rehabilitation. A
254 field campaign for ground truthing was conducted on March 17, 2021 to evaluate the
255 digitization quality of the drainage network. The head and mouth locations of some
256 channels were surveyed with dGPS. Assuming dGPS data as true control points, we
257 estimate the accuracy of our digitalization by calculating the root mean square error
258 (RMSE) . Since the last public topography covering the entire mine dates to 2018 (Table
259 1), we measured head and bottom locations in those channels experiencing no change
260 between 2018 and the present. Check points are shown in Figure 3. We conclude that
261 our digitalization has an average planimetric accuracy of 9 m.

262 The two LiDAR-ALS topographies were also used to analyze the most critical site in
263 terms of geomorphic instability in the “ α ” zone. They were transformed to DEMs and a
264 comparison between them through a DoD was obtained using the GCD methodology
265 (Wheaton et al., 2010) and software (GCD, 2018) to calculate the earth eroded in terms
266 of volume, depth and upstream migration. DoD analyses produced volume data and
267 images of erosion-deposition zones. Having detected the rapid evolution of the referred
268 gully area, a final survey with dGPS was carried out over the main active gullies in 2020
269 and was also processed with GCD software. The SfM-UAV topography survey obtained
270 on 15.04.2018 was used to obtain the base topography for the geomorphic design of the
271 “ β ” zone.

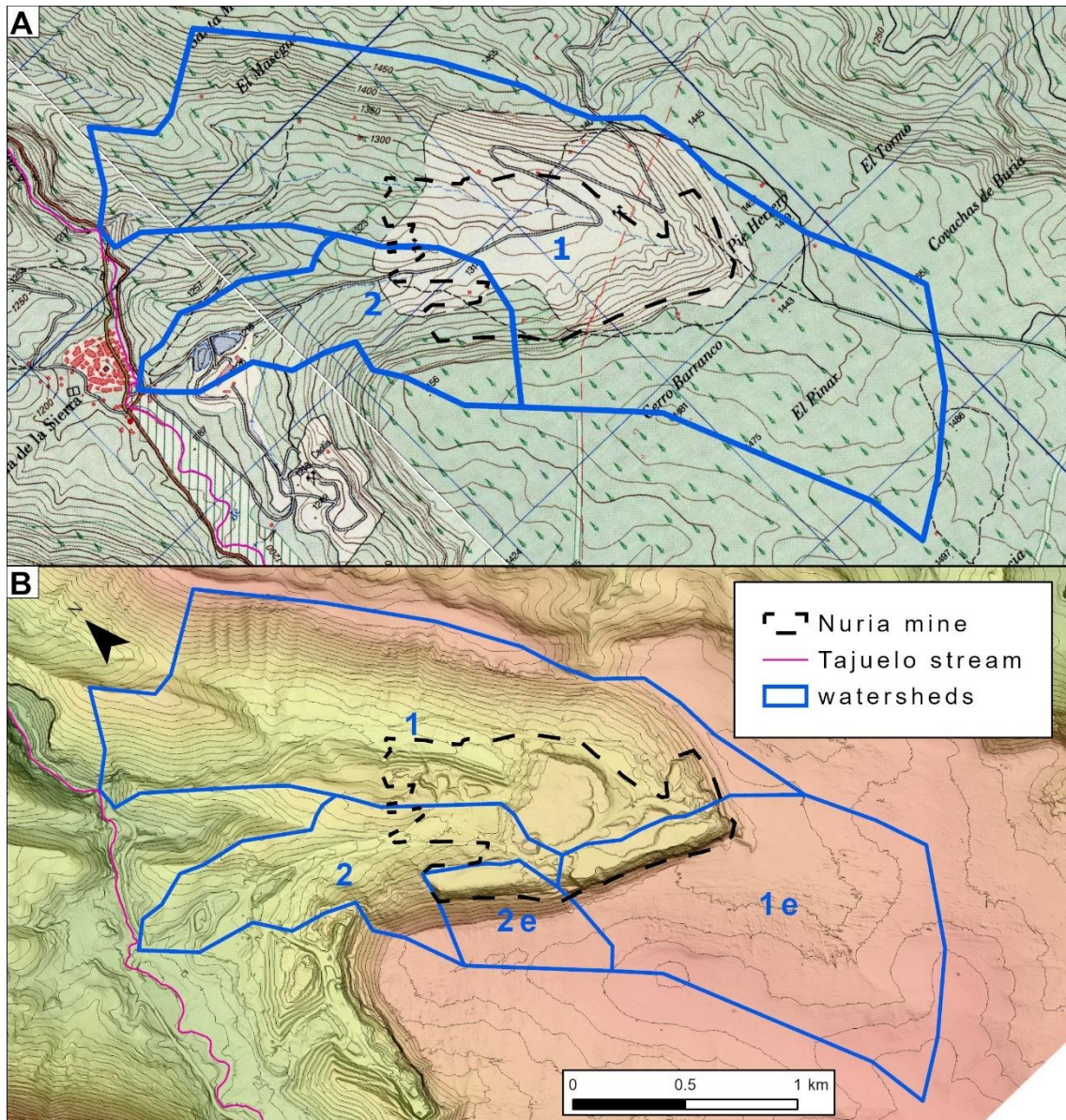
272 *2.3. Fluvial Geomorphic Rehabilitation*

273 A geomorphic approach was used to rehabilitate the damaged terraces in zone “ β 2”.
274 Since some sectors of zone “ β 1” terraces have not shown a significant sign of erosion
275 (Fig. 1), the geomorphic design is to be selectively adapted to these pre-existent
276 terraces. Hence, a mixed (hybrid) approach is applied to this case: the external terraces
277 were rebuilt (1.5 ha) and a geomorphic design based on the GeoFluv method and the
278 Natural Regrade software was planned for the highest part (3.6 ha).

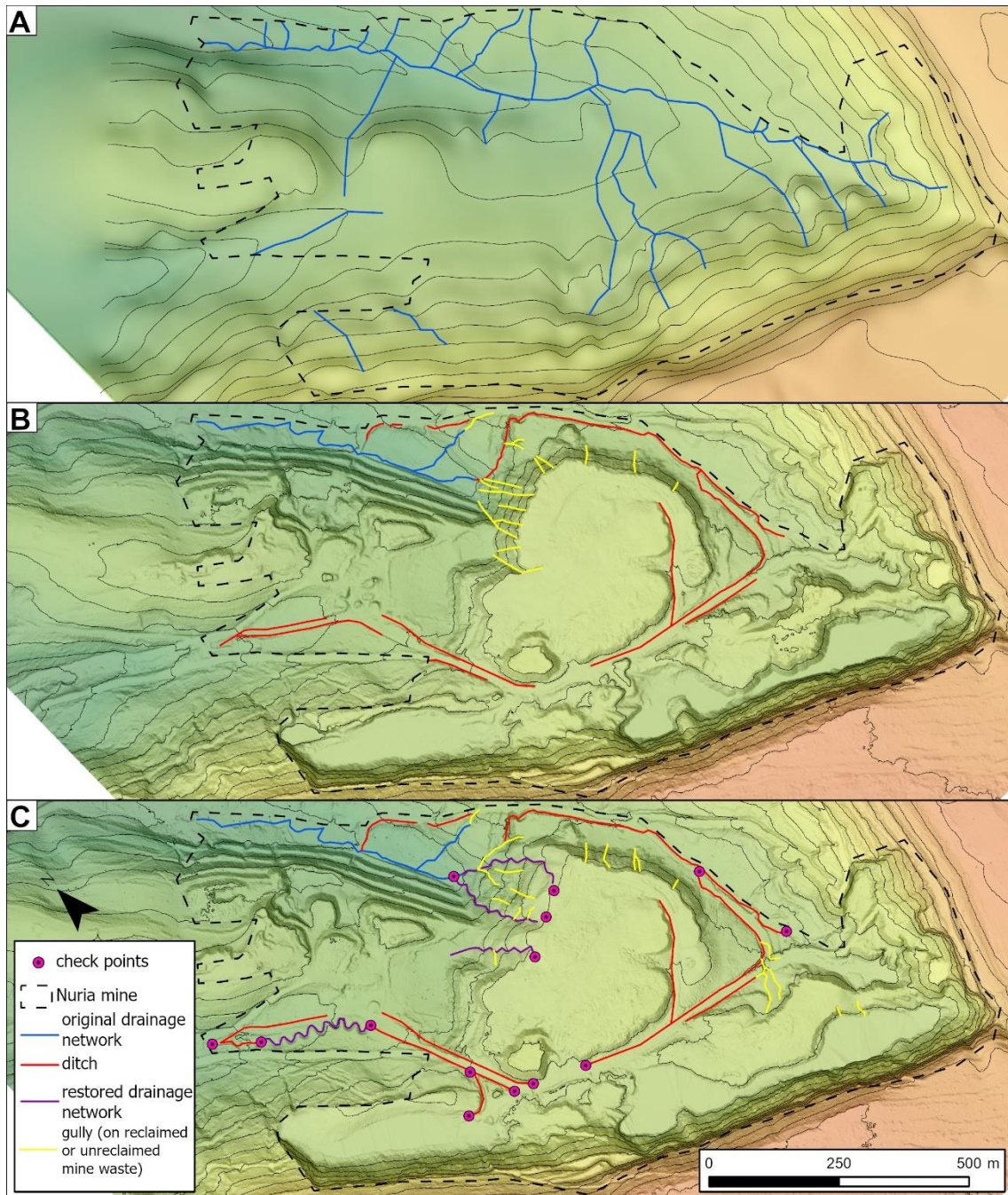
279 **3. Results**

280 *3.1. Temporal catchment and drainage network evolution in the Nuria mine*

281 The Nuria mine, located in the intermediate part of two sub-catchments of the Tajuelo
282 stream, drained water from 449 ha before mining activity ensued. These natural
283 catchments thereafter drained 62% of the catchment, the remaining area forming two
284 endorheic sub-catchments draining to ponds located at the bottom of the pits at the
285 highwall toe (Fig. 2). The drainage network developed in three stages: before the mining
286 activity in 1984 at the pre-mining stage; near the end of mining activity during 2009-2010
287 with the drainage network based on ditches and gullies; and, after eight years that natural
288 processes shaped the drainage network and undertaking three geomorphic
289 stabilization/rehabilitation projects (Fig. 3 and Table 2). In 1984 the drainage network
290 had a fourth stream order and a typical dendritic shape. It was modified by the mining
291 activity, which removed the upper part of the network and introduced straight artificial
292 drainage ditches mainly at the edges of the mine. Some gullies also appeared within
293 zones having no drainage. In 2018 new gullies grew and others were stabilized by
294 geomorphic rehabilitation, reshaped into new fluvial channels with zig-zag and
295 meandering shapes, based on local natural analogues (Zapico et al., 2020).



296
 297 Figure 2. Catchment evolution in the Nuria mine: (A) 1984, before mining; (B) 2018, after
 298 mining; (1, 2) natural catchments; (1e, 2e) mining-modified endorheic catchments with
 299 ponds at the highwall toe. A 25,000 map and a DEM and contours are the background
 300 for each date.



301

302 Figure 3. Temporal change in drainage network and type of drainage lines around the
 303 Nuria mine: (A) 1984, (B) 2010 and (C) 2018. A DEM and contours are the background
 304 for each map.

305

306

307

308

309

310

311

312

313

314 Table 2: Temporal variation of drainage network length and density in the Nuria mine.

	1984			2010			2018		
	length		density	length		density	length		density
	m	%	m ha ⁻¹	m	%	m ha ⁻¹	m	%	m ha ⁻¹
original (natural) drainage network	5,360	100	67	756	17	10	735	13	9
artificial ditches	0	0	0	2,910	64	36	2,950	53	37
restored drainage ¹	0	0	0	0	0	0	973	18	12
gully ²	0	0	0	872	19	11	905	16	11
total	5,360	100	67	4,540	100	57	5,560	100	69

315

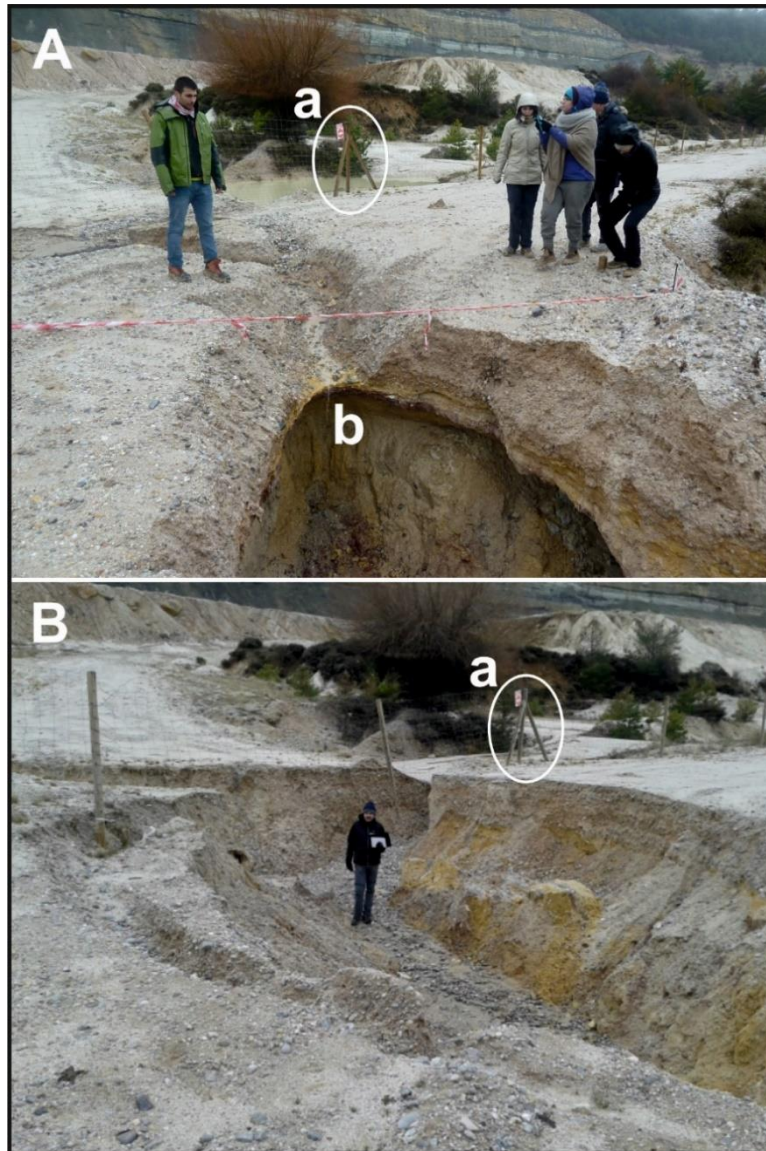
316 ¹ drainage network by Fluvial Geomorphic Rehabilitation

317 ² on reclaimed or unreclaimed mine waste

318

319 *3.2. Headcutting gully erosion migrating towards the ponds*

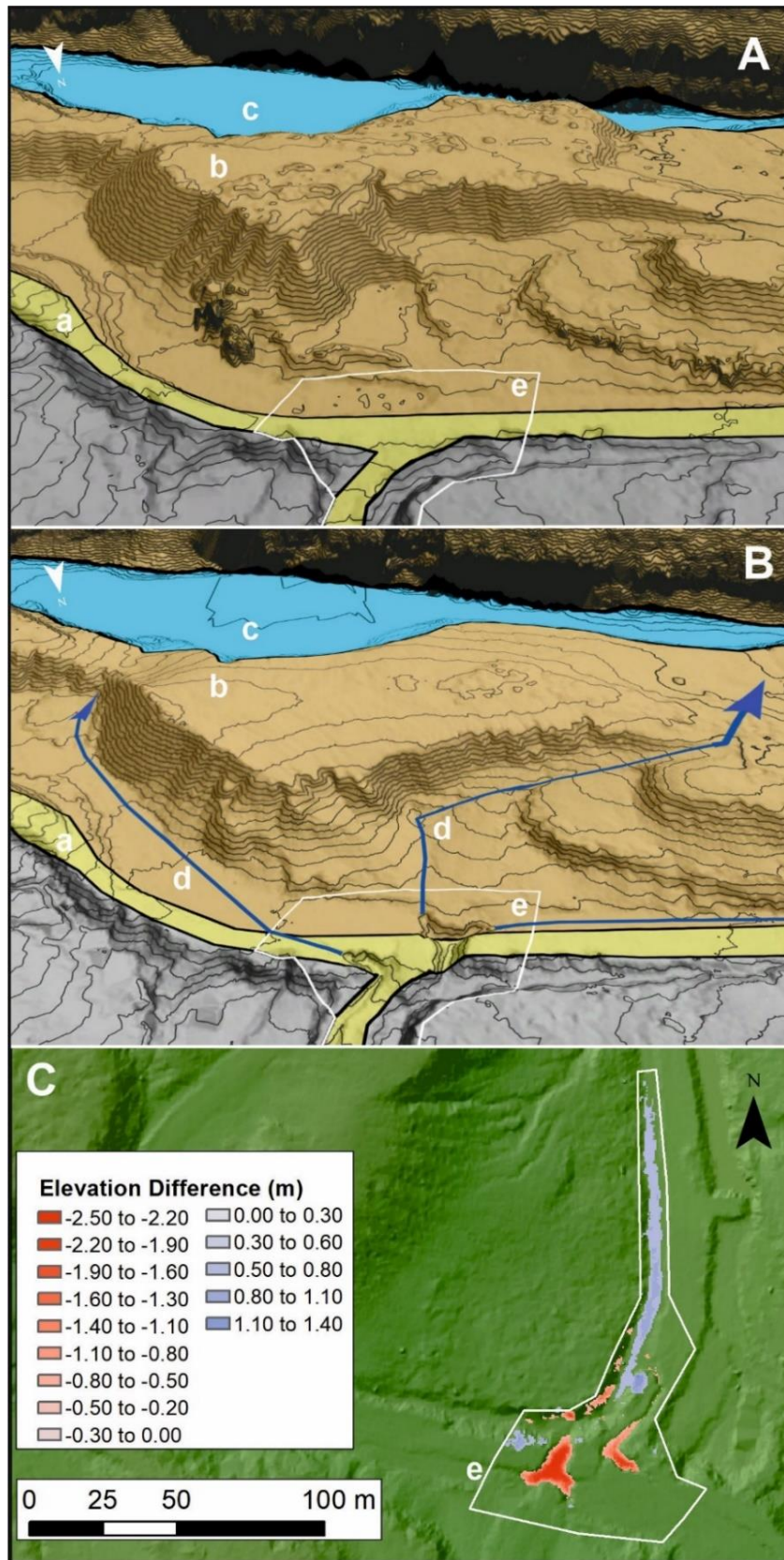
320 Although several efforts were undertaken to rehabilitate and stabilize the Nuria mine in
 321 zones “β” and “δ”, a significant surface, zone “α”, remained unstable. Here, frequent
 322 rilling and gulying erosion caused watercourse damage, producing high sediment yields
 323 and threatening the stability of the mine. The most hazardous zone is located
 324 downstream of one pond (yellow channels on the bottom right of Fig. 3C). Here, a road
 325 was dissected by the headcut migration of a knickpoint, initially advancing from the road
 326 ditch toward a series of ponds located at the base of a highwall (Fig. 4).



327
 328 Figure 4. Gully erosion cutting one of the roads in the Nuria mine. (A) knickpoint (b)
 329 migrating upstream (January 2016) and (B) erosion bisecting the road (February 2017).
 330 (a) the position of a wooden pole is used as reference. Modified from Hancock et al.
 331 (2020).

332

333 This gulying of the mine roadway was quantified by using the 2010-2018 LiDAR-ALS
 334 topographies (Fig. 5). The knickpoint advanced 25 m during 7.5 years having a 1.3 m
 335 average depth, maximum 2.5 m. This gully advanced an annual average rate of 3.3 m
 336 during the measurement period. This process can be clearly identified in the profiles of
 337 Fig. 6. Considerable (400 m³) sediment was eroded from the road, of which 300 m³ were
 338 deposited in a downstream ditch. The remaining sediment was transported downstream.

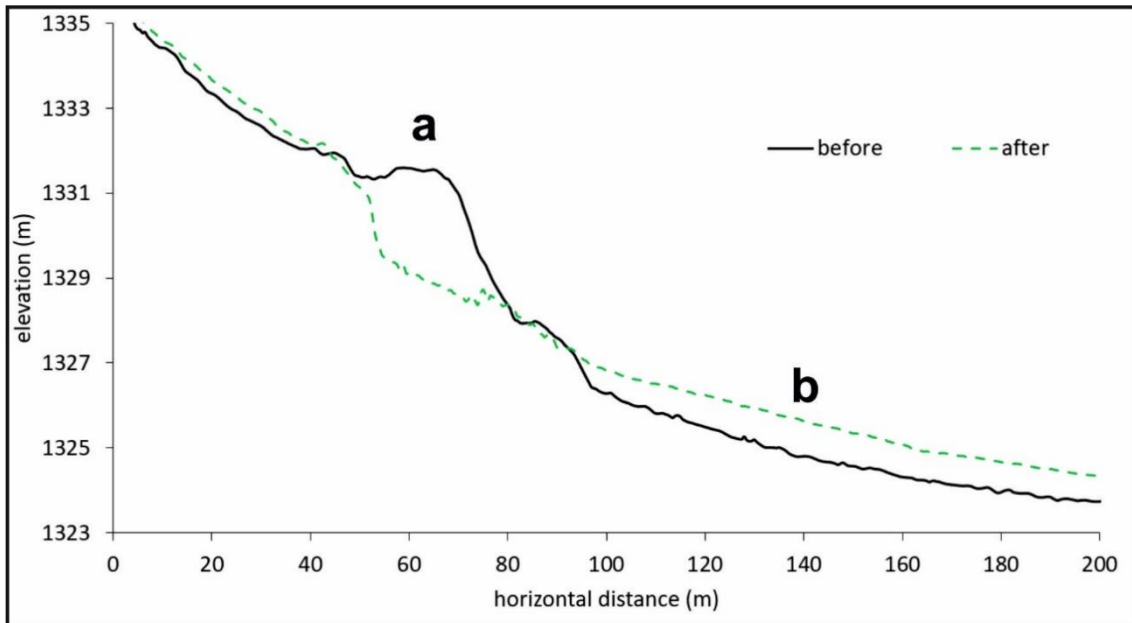


339

340 Figure 5. Topography before (A, 2010) and after (B, 2018) gully development. (C) DoD
 341 showing (a) unpaved road; (b) area between the ponds and the unpaved road; (c) pond;

342 (d) likely evolution of gully erosion; (e) polygon used to calculate the DoD in the gullied
343 area. The arrows in B show the direction of knickpoint migration.

344



345
346 Figure 6. Profile of gully erosion (a) and deposition (b) in the unpaved road and ditch
347 (see Figure 4).

348

349 To reassess the high erosive activity which took place between 2010 and 2018 (Fig. 5),
350 a new survey was conducted in 2020. The comparison between the 2020 and 2018
351 topographies shows that the left gully knickpoint (Fig. 5, B) advanced 53 m with a 0.8 m
352 average depth, resulting in a 26.5 m/yr average biannual advance. This gully activity
353 caused considerable (261 m³) erosion and deposition (64 m³), transporting 197 m³ of
354 sediment downstream.

355 3.3. Sustainable drainage system reconstruction

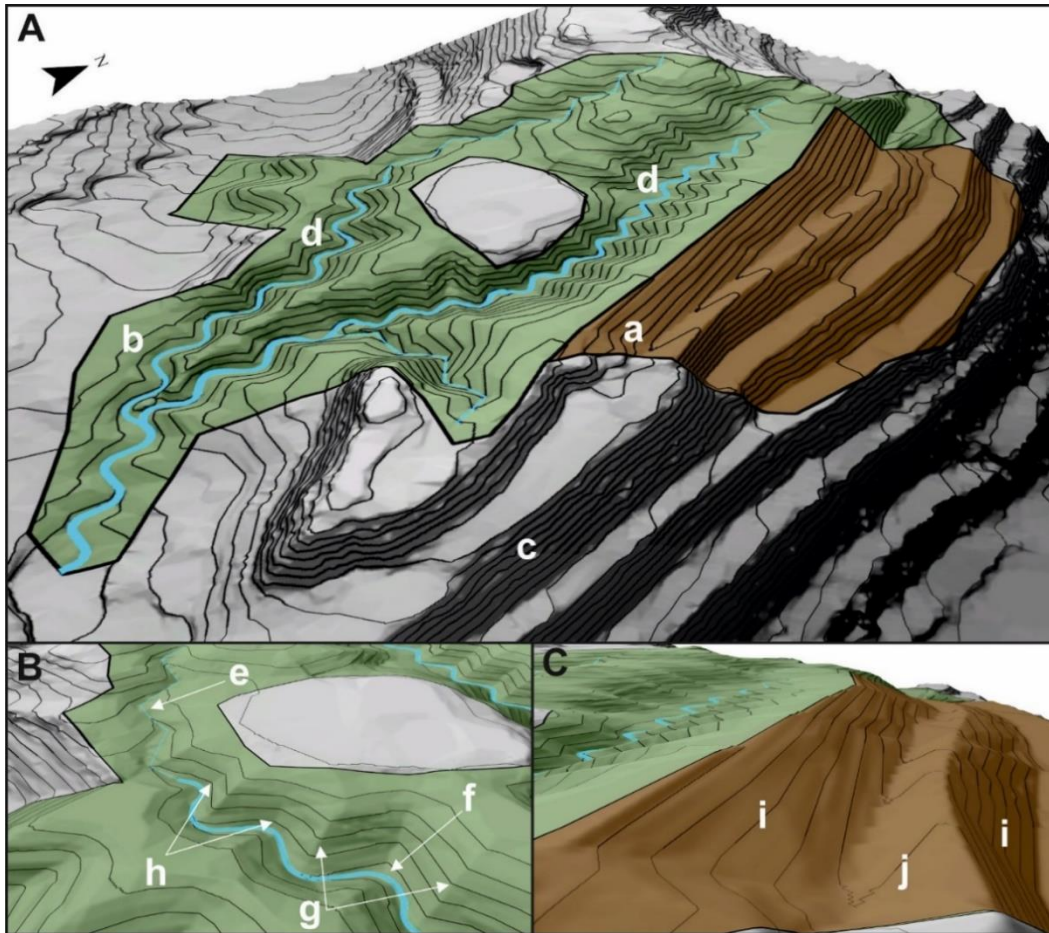
356 A detailed topography was surveyed using the SfM-UAV procedure (Fig. 7) to represent
357 the initial condition of the area. A geomorphic design was generated for the upper part
358 of the non-reclaimed area (Fig. 8) based on that topography and the parameters
359 measured in a local natural analogue. The channels have a zig-zag (slope > 4%) and
360 meander (slope < 4%) shapes; convex-concave hillslopes and concave swales were
361 added to the design. One channel is tributary to another, ending in a pond that operates

362 as base level. The channel slope varies (0 - 13 %); the entire reclaimed area has an
363 average 22% slope. The external terraces were also designed to be adapted to the
364 surrounding hillslopes (Fig. 7). The original terraces were very steep (50-60%), whereas
365 those designed are gentler (30-45%). Berm width varies in the range 7-13 m, having an
366 8% inverted gradient. This inverted gradient berm is a key issue for terrace preparation,
367 preventing water flowing from the next slope, thereby triggering rill and gully erosion.



368

369 Figure 7. Tiled model textured and contour view of the topography surveyed with SfM-
370 UAV on 15.04.2018.



371

372 Figure 8. A series of 3D views of the geomorphic and terrace rehabilitation design for “a”
 373 waste dump in the Nuria mine: general (A) and details (B and C). (a) reclaimed area in
 374 terraces; (b) geomorphic rehabilitation; (c) original surrounding topography; (d) main
 375 channels with zig-zag (e) and meander (f) patterns; (g) convex-concave sub-ridges; (h)
 376 concave swales; (i) outslope; (j) berm with inverted gradient.

377 The project area will be finalized by spreading a 1-m depth of carbonate colluvium and
 378 20 cm of topsoil. These thicknesses will be larger for the terraces, 2 m and 1 m
 379 respectively, owing to their higher gradient. The surface will be seeded with a mix of local
 380 herbaceous ground cover and shrubs. The rehabilitation started in the middle of 2018
 381 and currently the third terrace is almost finished. Once terrace construction ends, the
 382 final geomorphic design will be built with proper equipment (an excavator and a D6
 383 bulldozer). Altogether 190,000 m³ of waste material, 57,000 m³ of carbonate colluvium
 384 and 14,500 m³ of topsoil will be used in the rehabilitation.

385 **4. Discussion**

386 Here we first-ever carried out a full multi-temporal study of the evolution of the drainage
387 network density in a reclaimed mining area with historic maps and HRTs. We also
388 quantified the magnitude of the main gullying process of the mine, showing how the
389 absence of proper drainage density produces areas prone to flash flooding and
390 landslides. We also propose to restore an unstable area by creating a functional
391 catchment with natural shapes, including concave channels and convex-concave
392 hillslopes, with the novelty that it is adapted to a restored terraced area.

393 *4.1. Long-term catchment and drainage network evolution*

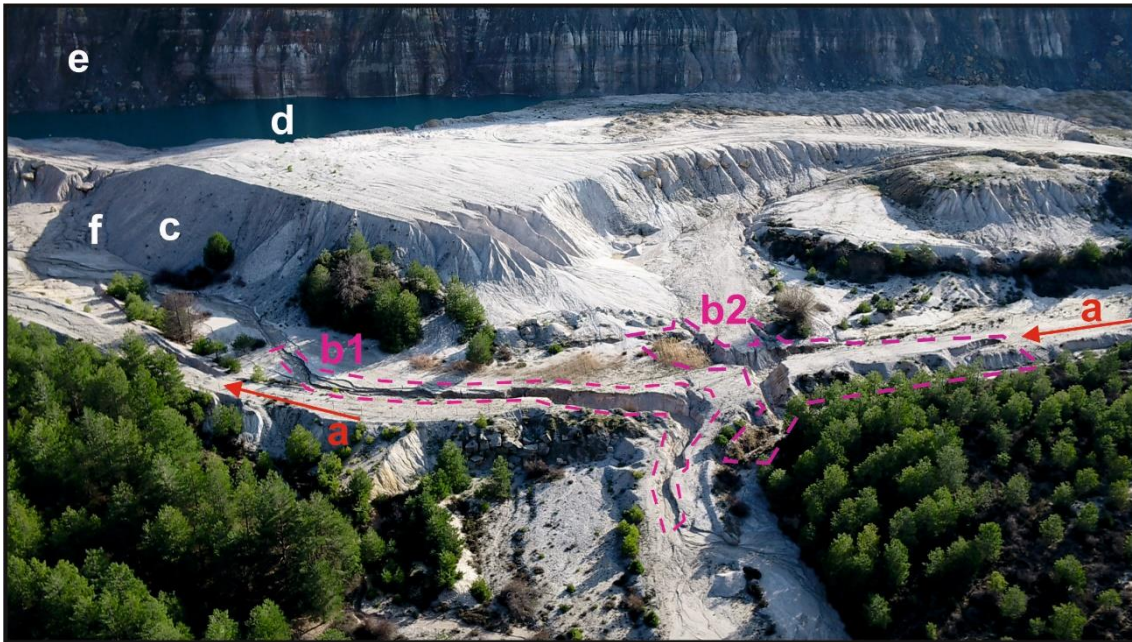
394 Topographic transformations always occur in mined areas. Among these, drainage
395 layouts can be disturbed by changing the spatial pattern of divides, either forming
396 endorheic basins, or modifying the main and secondary divides. The Nuria mine
397 exemplifies this impact: prior to mining this valley had a subtle divide between the
398 Matalascabras and the Carrascalejo valleys. Mining displaced this intra-valley divide
399 while the excavation at the foot of the mine highwall created endorheic basins draining
400 to several artificial ponds at the bottom of the pits (Fig. 2). These endorheic catchments
401 retain water from more than one third of the pre-mining area affected by the Nuria mine.
402 Despite the addition of ditches, mining activity decreased the pre-mine drainage density
403 (from 67 to 46 m ha⁻¹ — altogether a 31% reduction excluding gullies) by obliterating
404 most of the drainage network. This magnitude of reduction 18 - 84% depending on the
405 studied catchments, was also documented elsewhere (Kite et al., 2004). Such a
406 reduction in drainage density could be larger, because agricultural practises conducted
407 prior to the 1984 source map 'erased' a portion of the original natural drainage lines, by
408 filling the head of channels. However, the magnitude of this underestimation is unknown.
409 Sánchez-Donoso et al. (2020) estimated 5-7% reductions by this factor. The pre-mine
410 drainage density also reflects a drainage development on consolidated materials.
411 However, the Nuria mine changed the physical properties of most of the valley substrata,

412 from consolidated materials (sandstone and limestone) to unconsolidated sandy and
413 clayey mine waste deposits. The comparison of pre-mine and post-mine drainage
414 density are, therefore not directly comparable, as differences in substrata are to be
415 considered.

416 The change in materials used to restore to a pre-mining condition should be taken into
417 account in rehabilitation designs to adapt the drainage density to observed parameters
418 of a nearby drainage network (analogue) developed on materials similar to the mine
419 wastes (Hannan, 1984). The drainage density of this “reference area”, used as a valid
420 input for geomorphic mine rehabilitations in the Alto Tajo, is 110 m ha^{-1} (Zapico et al.,
421 2018). Based on this value and excluding gullies, the post-mine 2010 drainage density
422 was 58% lower than it should have been to ensure long term stability. Although some
423 gully areas were stabilized before 2018 (Zapico et al., 2020), the gully channel length in
424 2018 persists like that of 2010 because new gullies have formed, mostly in the southeast
425 of the mine, outside the current stable, geomorphically reclaimed areas (Fig. 3).

426 *4.2. Long and short-term gully processes in the Nuria mine*

427 Gully erosion and landslides are the main threats of instability in worldwide active and
428 reclaimed surface mines (Reed and Kite, 2020). In the Nuria case, site drainage system
429 ditches dated 2010 are concentrated at the edges of the mine, leaving many areas with
430 no drainage, thereby leading to the onset of active gullying that alter mine stability and
431 increase sediment yields. The determination of the average gully migration in the main
432 Nuria mine and its acceleration are evident (Fig. 9). Continued gully headcutting may
433 capture the ponds, triggering flash floods, with likely harmful effects downstream to the
434 natural park. Merely 130 m separate the active gully knickpoint and the weakest location
435 in the unconsolidated sand dam of one of the ponds. The sediment yields downstream
436 of the gully are similar to values reported by DoDs in a gully of an open-pit coal mine
437 dump associated with freeze-thaw cycles and meltwater erosion (Gong et al., 2019).



438
439 Figure 9. Oblique photo of the main active gully erosion in the Nuria mine threatening an
440 upstream pond (photographed on 26.03.2020). Road (a); left (b1) and right (b2)
441 headcutting gully erosion; earth —sand— dam (c) enclosing the pond (d); highwall (e);
442 weakest area in the earth —sand— dam (f). Photo by DGDRONE (2020).

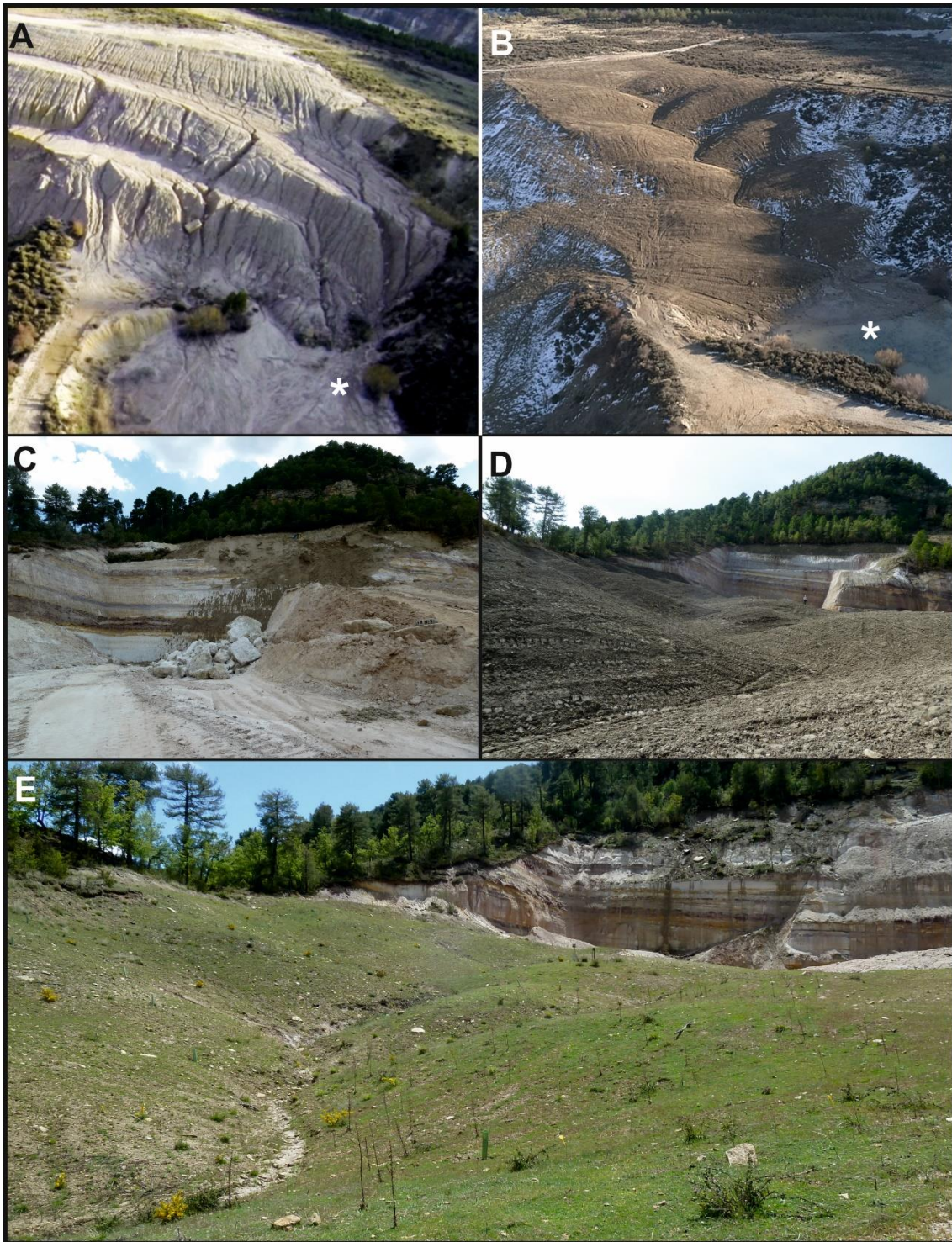
443 This adverse gullying phenomenon is well-known (Collier et al., 1970) and occurs in the
444 absence of a proper drainage system. Fluvial erosion creates an intruding channel
445 network, leading to sediment yields that risk loading the natural fluvial system (Zapico et
446 al., 2017), and the destruction of sensitive structures such as roads or ponds. Additional
447 evidence of water reproducing natural fluvial processes in the mine is the main gully
448 profile becoming concave (Fig. 6). Gullies can also appear linked to other mining zones,
449 such as the edge of reclaimed filled valleys and downstream of retention cells, as is
450 typical of coal mines of central Appalachia (Reed and Kite, 2020). Our observations
451 demonstrate a rise in the number of gullies with increased drainage area. Gully
452 appearance due to drainage network removal is not exclusive to the mining industry, as
453 it also occurs due to other anthropogenic activities such as urbanization (de Albuquerque
454 et al., 2020), and the combination of both urbanization and agricultural practices (Sofia
455 et al., 2014). Therefore, introduction of functional, long-term and steady-state drainage
456 networks should be incorporated in both mining rehabilitation and other disciplines.

457 *4.3. Restoring a drainage network through geomorphic rehabilitation*

458 Since 2018 a new geomorphic rehabilitation project using GeoFluv methodology is
459 recovering a formerly terraced zone in the Nuria mine. The novelty in this case is that it
460 is a first instance that such a methodology is being adapted to pre-existing terraces. Our
461 design demonstrates how a geomorphic rehabilitation approach can be adapted to
462 traditionally constructed rehabilitation. Using a catchment as the main rehabilitation unit
463 (Hannan, 1984), a new landscape was designed accounting for the often suggested
464 features: appropriate drainage density, channels with concave profiles without
465 knickpoints and bankfull cross sections, and convex-concave hills (Stiller et al., 1980).
466 Other important hydrological principles included in this design are: the constructed
467 drainage density is adapted to the final rehabilitation landscape in terms of sediment type
468 and slope; and, with increase in drainage area, channel length and cross-sections also
469 increase (Hannan, 1984). These features also characterize another geomorphic
470 rehabilitation project undertaken in the Nuria mine in 2017 (Fig. 10, A and B). Here a
471 terraced waste dump experienced severe rill and gully erosion, preventing the support
472 of a new ecosystem Fig. 10, C-D shows the evolution of the first geomorphic
473 rehabilitation done in the Alto Tajo Natural Park in 2011 (Zapico et al., 2018).

474 A recent study proposes overcoming the lack of a proper drainage system in slope
475 surfaces with terraces by introducing many straight intercepting drains following the
476 maximum slope, instead of few ditches following the contours and a reinforced concrete
477 lattice (Kou et al., 2020). This approach assimilates two important features of Fluvial
478 Geomorphic Rehabilitation: increase the drainage density and avoid concentrating water
479 and sediment. However, the Kou et al. (2020) system is still based on artificial landforms,
480 which do not ensure long-term stability.

481



482
 483 Figure 10. Another geomorphic rehabilitation surfaces in mines of the Alto Tajo: Nuria
 484 (before, A; after, B) and Machorro (before, C; after, D; present, E). (*) pond position is
 485 used as reference. A and B oblique photos by DGDRONE.

486 Since a rehabilitation project should be based on the construction of detailed natural
 487 shapes adapted to the surrounding area, it requires accurate topographic information
 488 (Stiller et al., 1980). We conducted a UAV-SfM survey with a 4.4 cm vertical accuracy

489 (Table 1) as the base of our design. It is lower than that of other topographies surveyed
490 in the area (Zapico et al., 2020, 2018), because the control/check points were measured
491 with a differential GPS instead of a total station, and flight height was larger. This error
492 is present in the final design topography.

493 *4.4. Next steps to fully stabilize and restore the Nuria mine*

494 The risks of the Nuria mine arose from the lack of a proper closure plan. The terraced
495 waste dumps occupying half of the mine have been or are being stabilized and restored.
496 However, the rest of the mine (“ α ” in Fig. 1) is experiencing severe erosion by an
497 unstable, interim drainage network, thereby threatening the long-term stability of the
498 mine. Not only is it increasing drainage density, but it is also shaping channels with
499 predominately concave profiles that can affect roads and ponds in the Nuria mine. If
500 erosion reaches a pond, a flash flood may be generated, moving to the two downstream
501 waste dumps, thereby potentially creating a catastrophic massive earth movement.
502 Hence, urgent measures are required to restore the “ α ” zone.

503 Since geomorphic rehabilitation is based on introducing a locally adapted channel
504 network, future plans should be based on this preferred methodology. Expert geomorphic
505 designs can reduce erosion by as much by half in comparison to conventional designs
506 (Hancock et al., 2019). Specifically, ponds located at the highwall base should be
507 removed by filling them with waste material and regrading. The final configuration should
508 be similar to the geomorphic rehabilitation in the nearby Machorro mine (Zapico et al.,
509 2018). Furthermore, the area between the ponds and the waste dumps should also be
510 regraded to introduce a drainage network and avoid the present rill and gully erosion.
511 Apart from stabilizing the restored areas, geomorphic rehabilitation also allows better
512 diversity of plant communities compared to traditional rehabilitation, characterized by
513 uniform topography and linear slopes of post-mining sites (Fleisher and Hufford, 2020).
514 The average gentle slope of the design will also optimize soils moisture availability,
515 improving the development of vegetation (Vidal-Macua et al., 2020).

516 Unacceptable environmental practices and an inadequate closure plan involved the
517 rejection of a new concession extension in the Nuria mine; authorities did not return the
518 bond release to the mining owners. This guarantee was confined to meet expenses to
519 stabilize the rotational landslide. The current rehabilitation occurring in another waste
520 dump is being carried out by the only active mining company in the area, by jointly
521 planning with the mining administration and the natural park authorities an attempt to
522 gain stability of the entire mine through several compensatory mitigation measures. This
523 agreement enables the mining company to access a place to stockpile part of its wastes
524 with the commitment to regrade the final topography with geomorphic rehabilitation,
525 thereby removing stability risks. Owing to the high cost of earth movement and
526 completion of bond release, this type of collaboration between authorities and the local
527 active mining company may be extended to stabilize and restore the rest of the mine.

528 *4.5. The false dilemma between a geomorphic (natural drainage recovery) or soil focus*
529 *in mine rehabilitation*

530 The use of a geomorphic landform design approach in mine rehabilitation with respect
531 to soils - either by using soil erosion modelling, or protocols for handling the soil - also in
532 mine rehabilitation is still often raised as a disjunctive question. One must often choose
533 between two supposedly mutually exclusive options – either use fluvial geomorphic
534 landform design with a natural drainage recovery, or else use soil erosion modelling,
535 thereby improving physico-chemical properties. However, this is a false dilemma, since
536 both approaches are required and are complementary. Several studies have
537 demonstrated that joint use of geomorphic landform design and landscape evolution
538 modeling provide complementary capabilities to enhance mine rehabilitation (e.g.,
539 Hancock et al., 2019). The cause of this false dilemma appears to lie in the understanding
540 that both elements (drainage network and soils) operate at different scales. The drainage
541 basin operates at a landscape scale, whereas soil operates at the catena, hillslope scale;
542 both are compatible. As demonstrated by the Nuria example, a specific drainage density
543 is needed to naturally drain that landscape, independent of soil treatment.

544 This reasoning goes beyond: we argue that without a geomorphic approach of
545 reconstructing drainage systems equivalent to natural ones in order to repair land and
546 ecosystems disturbed by mining, recovery will remain partial, and should not be termed
547 either 'ecologic' or 'landscape' rehabilitation. Avoiding soil erosion is indeed a condition,
548 and key issue, to mine rehabilitation (Vidal-Macua et al., 2020). But this is insufficient,
549 nor is it currently the best possible practice. The reasons for this insufficiency are listed
550 hereafter: (a) most functional ecologic processes occur on the Earth's land surface at a
551 watershed scale, driven by hillslope runoff and fluvial processes: (b) visual blending of
552 waste dumps with the surrounding is nowadays a major issue for society. Merely
553 avoiding erosion is no longer sufficient for most government agencies, local inhabitants
554 and visitors to a mine.

555 **5. Conclusions**

556 A very defective mining operation and the lack of a proper closure plan in the Nuria mine
557 are threatening one of the most biodiverse natural parks in Spain, the Alto Tajo. As a
558 consequence of the mining activity the original drainage network was considerably
559 reduced and the new pit configuration, with three ponds filling topographic depressions,
560 modified the original catchments forming two new endorheic sub-catchments. One of
561 these ponds is enclosed by an unconsolidated dam and it is threatened by a rapidly
562 advancing gully, which was created by the redevelopment of the obliterated drainage
563 network. This lack of a locally congruous drainage system is being overcome through
564 the application of a Fluvial Geomorphic Rehabilitation approach, creating a new,
565 dynamically equilibrated landscape. This is organized in a main catchment and sub-
566 catchments with a drainage density adapted to the materials and slopes of the
567 rehabilitated area, and with natural features such as concave channels and convex-
568 concave hills adapted to preexisting terraces. The current Nuria mine rehabilitation is a
569 good example of the compensatory measures between other active mining companies

570 and local authorities, which can be explored to apply corrective action to adequately
571 rehabilitate abandoned mine sites.

572 As a global contribution, we provide here an example of mine rehabilitation
573 demonstrating that, with a (geomorphic) focus on reestablishing drainage systems
574 equivalent to natural ones, mine rehabilitation: (a) is stable; (b) natural recovery can be
575 complete, and should either be termed 'ecologic' or 'landscape' rehabilitation.

576

577 **Acknowledgements**

578 This study was funded by (i) the Ecological Restoration Network (REMEDINAL TE-CM)
579 of the Madrid Community (P2018/EMT-4338) ; (ii) the postdoctoral grant Torres Quevedo
580 (cofounded by the Spanish Ministry of Science, Innovation and Universities, and Diseño
581 y Desarrollo Minero SL company) to Ignacio Zapico (PTQ-17-09404). We thank S.
582 Nyssen, M. Tejedor, C. Martín, Á. Vela, R. Ibáñez, R. Ruiz, J.A. Lozano, Á. Moya, J.
583 González, Q. Rubio, J. de la Villa, N. Bugosh, V. Lopez and the staff rangers of the Alto
584 Tajo Natural Park for their support. We especially thank David Gutiérrez (DGDRONE),
585 our drone pilot and aerial film maker, Melanie Ball for English editing of the manuscript,
586 and Alfonsa Campos, general manager of DDM SL.

587 **References**

- 588 Bugosh, N., Epp, E., 2019. Evaluating sediment production from native and fluvial
589 geomorphic-reclamation watersheds at La Plata Mine. *CATENA* 174, 383–398.
590 <https://doi.org/10.1016/J.CATENA.2018.10.048>
- 591 Carabassa, V., Montero, P., Crespo, M., Padró, J.-C., Pons, X., Balagué, J., Brotons,
592 L., Alcañiz, J.M., 2020. Unmanned aerial system protocol for quarry restoration
593 and mineral extraction monitoring. *J. Environ. Manage.* 270, 110717.
594 <https://doi.org/10.1016/J.JENVMAN.2020.110717>
- 595 Carrivick, J.L., Smith, M.W., Quincey, D.J., 2016. New analytical methods in earth and
596 environmental science: Structure from Motion in the geosciences.

597 Collier, C., Pickering, R., Musser, J., 1970. Influences of strip mining on the hydrologic
598 environment of parts of Beaver creek basin, Kentucky, 1955-66. US Geol. Surv.
599 Prof. Pap. <https://doi.org/10.3133/pp427d>

600 Cucchiaro, S., Cavalli, M., Vericat, D., Crema, S., Llana, M., Beinat, A., Marchi, L.,
601 Cazorzi, F., 2018. Monitoring topographic changes through 4D-structure-from-
602 motion photogrammetry: application to a debris-flow channel. Environ. Earth Sci.
603 77, 0. <https://doi.org/10.1007/s12665-018-7817-4>

604 de Albuquerque, A.O., de Carvalho Júnior, O.A., Guimarães, R.F., Gomes, R.A.T.,
605 Hermuche, P.M., 2020. Assessment of gully development using geomorphic
606 change detection between pre- and post-urbanization scenarios. Environ. Earth
607 Sci. 79, 232. <https://doi.org/10.1007/s12665-020-08958-9>

608 ESRI, 2020. ArcGIS Pro 2.5.1.

609 Fleisher, K.R., Hufford, K.M., 2020. Assessing habitat heterogeneity and vegetation
610 outcomes of geomorphic and traditional linear-slope methods in post-mine
611 reclamation. J. Environ. Manage. 255, 109854.
612 <https://doi.org/10.1016/J.JENVMAN.2019.109854>

613 Garbarino, E., Orveillon, G., Saveyn, H., Barthe, P., Eder, P., 2018. Best Available
614 Techniques (BAT) reference document for the management of waste from
615 extractive industries in accordance with directive 2006/21/EC. Publications Office
616 of the European Union, Luxemburg.
617 https://doi.org/https://doi.org/10.36487/ACG_rep/1915_121_Howard

618 GCD, 2018. Geomorphic Change Detection Software, Version 7.1.1.0 [WWW
619 Document]. URL <http://gcd.riverscapes.xyz/> (accessed 9.1.18).

620 Gong, C., Lei, S., Bian, Z., Liu, Y., Zhang, Z., Cheng, W., Gong, C., Lei, S., Bian, Z.,
621 Liu, Y., Zhang, Z., Cheng, W., 2019. Analysis of the development of an erosion

622 gully in an open-pit coal mine dump during a winter freeze-thaw cycle by using
623 low-cost UAVs. *Remote Sens.* 11, 1356. <https://doi.org/10.3390/rs11111356>

624 Hancock, G.R., Duque, J.F.M., Willgoose, G.R., 2020. Mining rehabilitation – Using
625 geomorphology to engineer ecologically sustainable landscapes for highly
626 disturbed lands. *Ecol. Eng.* 155, 105836.
627 <https://doi.org/10.1016/J.ECOLENG.2020.105836>

628 Hancock, G.R., Duque, J.F.M., Willgoose, G.R., 2019. Geomorphic design and
629 modelling at catchment scale for best mine rehabilitation – The drayton mine
630 example (New South Wales, Australia). *Environ. Model. Softw.* 114, 140–151.
631 <https://doi.org/10.1016/J.ENVSOF.2018.12.003>

632 Hannan, J.C., 1984. *Mine rehabilitation: a handbook for the coal mining industry*,
633 Sydney. ed. New South Wales Coal Association.

634 Howard, E.J., Loch, R.J., Vacher, C.A. 2011. Evolution of landform design concepts.
635 *Mining Technology. Trans. Institutions Min. Metall. Sect. A Min. Technol.* 120,
636 112–117. <https://doi.org/10.1179/037178411X12942393517615>.

637 IGN, 1995. *Mapa Topográfico Nacional De España 1:25.000. Peralejos De Las*
638 *Truchas Hoja 539-2. Instituto Geográfico Nacional, Madrid. (in Spanish).*

639 Katpatal, Y.B., Patil, S.A., Singh, C.K., 2017. Estimation of sediment yield within mining
640 watershed to assess impact of mine dumps using satellite data: modified
641 approach. *J. Environ. Eng.* 143, 05017004.
642 [https://doi.org/10.1061/\(ASCE\)EE.1943-7870.0001261](https://doi.org/10.1061/(ASCE)EE.1943-7870.0001261)

643 Kite, J.S., Smith, J., Rengers, F.K., Walker, J.C., 2004. Impacts of surface mining and
644 “AOC” reclamation on small streams and drainage network, in: Barnhisel, R.I.
645 (Ed.), *Proceedings American Society of Mining and Reclamation 21st Annual*
646 *National Conference. American Society of Mining and Reclamation, Lexington, pp.*

647 1120–1147. <https://doi.org/10.21000/JASMR04011120>

648 Kou, P., Xu, Q., Yunus, A.P., Dong, X., Pu, C., Zhang, X., Jin, Z., 2020. Micro-
649 topographic assessment of rill morphology highlights the shortcomings of current
650 protective measures in loess landscapes. *Sci. Total Environ.* 737, 139721.
651 <https://doi.org/10.1016/J.SCITOTENV.2020.139721>

652 López-Vinielles, J., Ezquerro, P., Fernández-Merodo, J.A., Béjar-Pizarro, M.,
653 Monserrat, O., Barra, A., Blanco, P., García-Robles, J., Filatov, A., García-
654 Davalillo, J.C., Sarro, R., Mulas, J., Mateos, R.M., Azañón, J.M., Galve, J.P.,
655 Herrera, G., 2020. Remote analysis of an open-pit slope failure: Las Cruces case
656 study, Spain. *Landslides* 1–16. <https://doi.org/10.1007/s10346-020-01413-7>

657 Lucieer, A., Jong, S.M. de, Turner, D., 2014. Mapping landslide displacements using
658 Structure from Motion (SfM) and image correlation of multi-temporal UAV
659 photography. *Prog. Phys. Geogr.* 38, 97–116.
660 <https://doi.org/10.1177/0309133313515293>

661 Martín-Moreno, C., Martín Duque, J.F., Nicolau Ibarra, J.M., Muñoz-Martín, A., Zapico,
662 I., 2018. Waste dump erosional landform stability – a critical issue for mountain
663 mining. *Earth Surf. Process. Landforms* 43, 1431–1450.
664 <https://doi.org/10.1002/esp.4327>

665 Martín Duque, J., Tejedor, M., Martín-Moreno, C., Nicolau, J., Zapico, I., 2019.
666 Geomorphic rehabilitation in Europe: recognition as best available technology and
667 its role in LIFE projects, in: Fourie, A., Tibbett, M. (Eds.), *Proceedings of the 13th*
668 *International Conference on Mine Closure*. Australian Centre for Geomechanics,
669 Perth, pp. 133–146.

670 McKenna, G.T., Dawson, R., 1997. Landscape engineering for sustainable
671 development, in: *The Geotechnical Society of Edmonton Third Annual*
672 *Symposium: Environmentally Friendly Technologies in Geotechnical Engineering*.

673 Edmonton.

674 Mossa, J., James, L.A., 2013. 13.6 Impacts of mining on geomorphic systems, in:
675 Shroder, J.F. (Ed.), *Treatise on Geomorphology*. Academic Press, San Diego, pp.
676 74–95. <https://doi.org/10.1016/B978-0-12-374739-6.00344-4>

677 PNOA, 2018. Plan Nacional De Ortofotografía Aérea, LiDAR De Castilla la–Mancha,
678 Vuelo De 2018. Instituto Geográfico Nacional, Ministerio de Fomento. (in
679 Spanish).

680 PNOA, 2009. Plan Nacional De Ortofotografía Aérea, LiDAR De Castilla la–Mancha,
681 Vuelo De 2009. Instituto Geográfico Nacional, Ministerio de Fomento (Accessed
682 06.12.2016). (in Spanish). <http://pnoa.ign.es/>.

683 Qcoherent, 2018. LP360 Advanced Level, Version 2018.1.57.7 [WWW Document].
684 URL <https://geocue.com/products/lp-360/>

685 Reed, M., Kite, S., 2020. Peripheral gully and landslide erosion on an extreme
686 anthropogenic landscape produced by mountaintop removal coal mining. *Earth*
687 *Surf. Process. Landforms* esp.4867. <https://doi.org/10.1002/esp.4867>

688 Ross, M.R. V., McGlynn, B.L., Bernhardt, E.S., 2016. Deep impact: effects of
689 mountaintop mining on surface topography, bedrock structure, and downstream
690 waters. *Environ. Sci. Technol.* 50, 2064–2074.
691 <https://doi.org/10.1021/acs.est.5b04532>

692 Sánchez-Donoso, R., Bugosh, N., Martín-Duque, J.F., 2020. Use of Remote Sensing
693 Tools to Measure a Fluvial Geomorphic Design-Input Parameter for Land
694 Reclamation. *Water* 12, 2378. <https://doi.org/10.3390/w12092378>

695 Sawatsky, L.F., Beersing, A., 2014. Configuring mine disturbed landforms for long-term
696 sustainability, in: *Proceedings of Mine Closure Solutions, 2014*. InfoMine, Ouro
697 Preto, Minas Gerais, Brazil, pp. 1–13.

698 SMCRA, 1977. Surface Mining Control and Reclamation Act, Public law, 95–87,
699 Statutes at Large, 91 Stat. 445, Federal Law, United States, Washington DC,
700 1977.

701 Sofia, G., Prosdocimi, M., Dalla Fontana, G., 2014. Modification of artificial drainage
702 networks during the past half-century: Evidence and effects in a reclamation area
703 in the Veneto floodplain (Italy). *Anthropocene* 6, 48–62.
704 <https://doi.org/10.1016/J.ANCENE.2014.06.005>

705 Stiller, D.M., Zimpfer, G.L., Bishop, M., 1980. Application of geomorphic principles to
706 surface mine reclamation in the semiarid west. *J. soil water Conserv.* 35, 274–
707 277. <https://doi.org/10.21000/JASMR18020061>

708 Tarolli, P., Sofia, G., CAO, W., 2018. The geomorphology of the human age, in:
709 Dellasala, D.A., Goldstein, M.I. (Eds.), *Encyclopedia of the Anthropocene*.
710 Elsevier, pp. 35–43. <https://doi.org/10.1016/B978-0-12-809665-9.10501-4>

711 Vidal-Macua, J.J., Nicolau, J.M., Vicente, E., Moreno-de las Heras, M., 2020.
712 Assessing vegetation recovery in reclaimed opencast mines of the Teruel coalfield
713 (Spain) using Landsat time series and boosted regression trees. *Sci. Total*
714 *Environ.* 717, 137250. <https://doi.org/10.1016/J.SCITOTENV.2020.137250>

715 Wheaton, J.M., Brasington, J., Darby, S.E., Sear, D.A., 2010. Accounting for
716 uncertainty in DEMs from repeat topographic surveys: improved sediment
717 budgets. *Earth Surf. Process. Landforms* 35, 136–156.
718 <https://doi.org/10.1002/esp.1886>

719 Xiang, J., Chen, J., Sofia, G., Tian, Y., Tarolli, P., 2018. Open-pit mine geomorphic
720 changes analysis using multi-temporal UAV survey. *Environ. Earth Sci.* 77, 220.
721 <https://doi.org/10.1007/s12665-018-7383-9>

722 Zapico, I., Laronne, J.B., Martín-Moreno, C., Martín-Duque, J.F., Ortega, A., Sánchez-

723 Castillo, L., 2017. Baseline to evaluate off-site suspended sediment-related mining
724 effects in the Alto Tajo Natural Park, Spain. *L. Degrad. Dev.* 28, 232–242.
725 <https://doi.org/10.1002/ldr.2605>

726 Zapico, I., Laronne, J.B., Meixide, C., Sánchez Castillo, L., Martín Duque, J.F., 2021.
727 Evaluation of sedimentation pond performance for a cleaner water production from
728 an open pit mine at the edge of the Alto Tajo Natural Park. *J. Clean. Prod.* 280,
729 124408. <https://doi.org/10.1016/J.JCLEPRO.2020.124408>

730 Zapico, I., Martín Duque, J.F., Bugosh, N., Laronne, J.B., Ortega, A., Molina, A.,
731 Martín-Moreno, C., Nicolau, J.M., Sánchez Castillo, L., 2018. Geomorphic
732 reclamation for reestablishment of landform stability at a watershed scale in mined
733 sites: The Alto Tajo Natural Park, Spain. *Ecol. Eng.* 111, 100–116.
734 <https://doi.org/10.1016/j.ecoleng.2017.11.011>

735 Zapico, I., Molina, A., Laronne, J.B., Sánchez Castillo, L., Martín Duque, J.F., 2020.
736 Stabilization by geomorphic reclamation of a rotational landslide in an abandoned
737 mine next to the Alto Tajo Natural Park. *Eng. Geol.* 264, 105321.
738 <https://doi.org/10.1016/J.ENGGEOL.2019.105321>

Figure 1

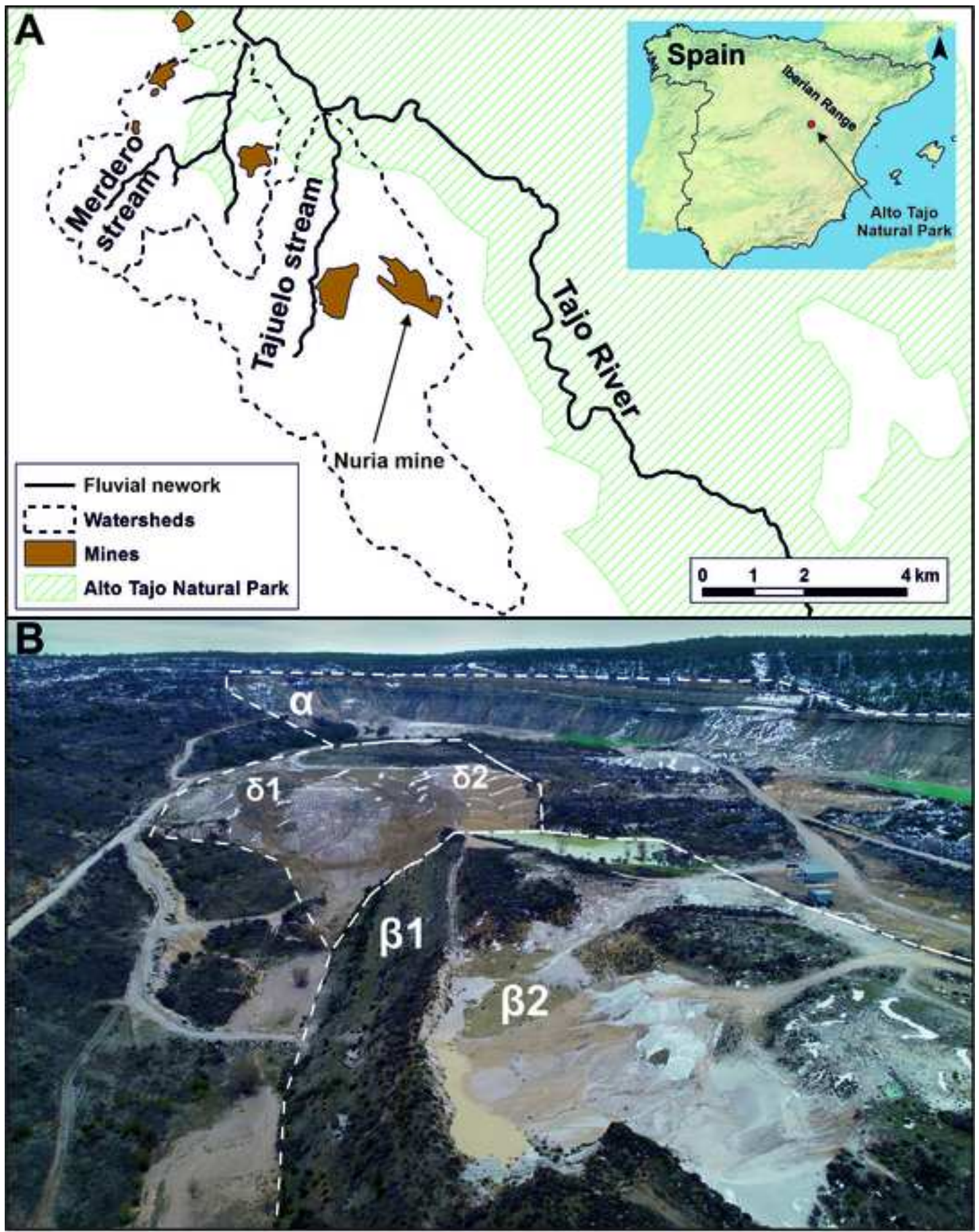


Figure 2

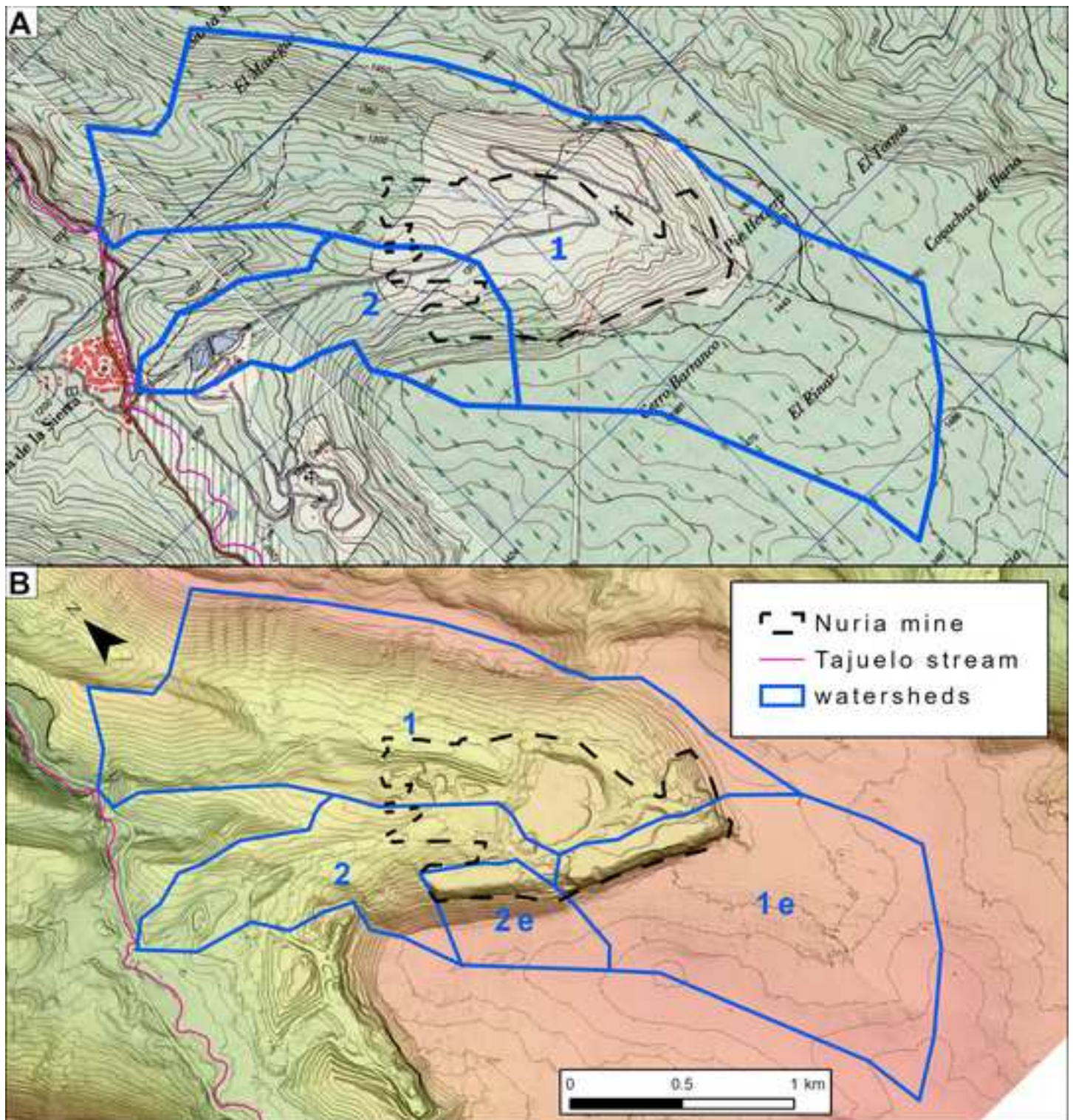


Figure 3

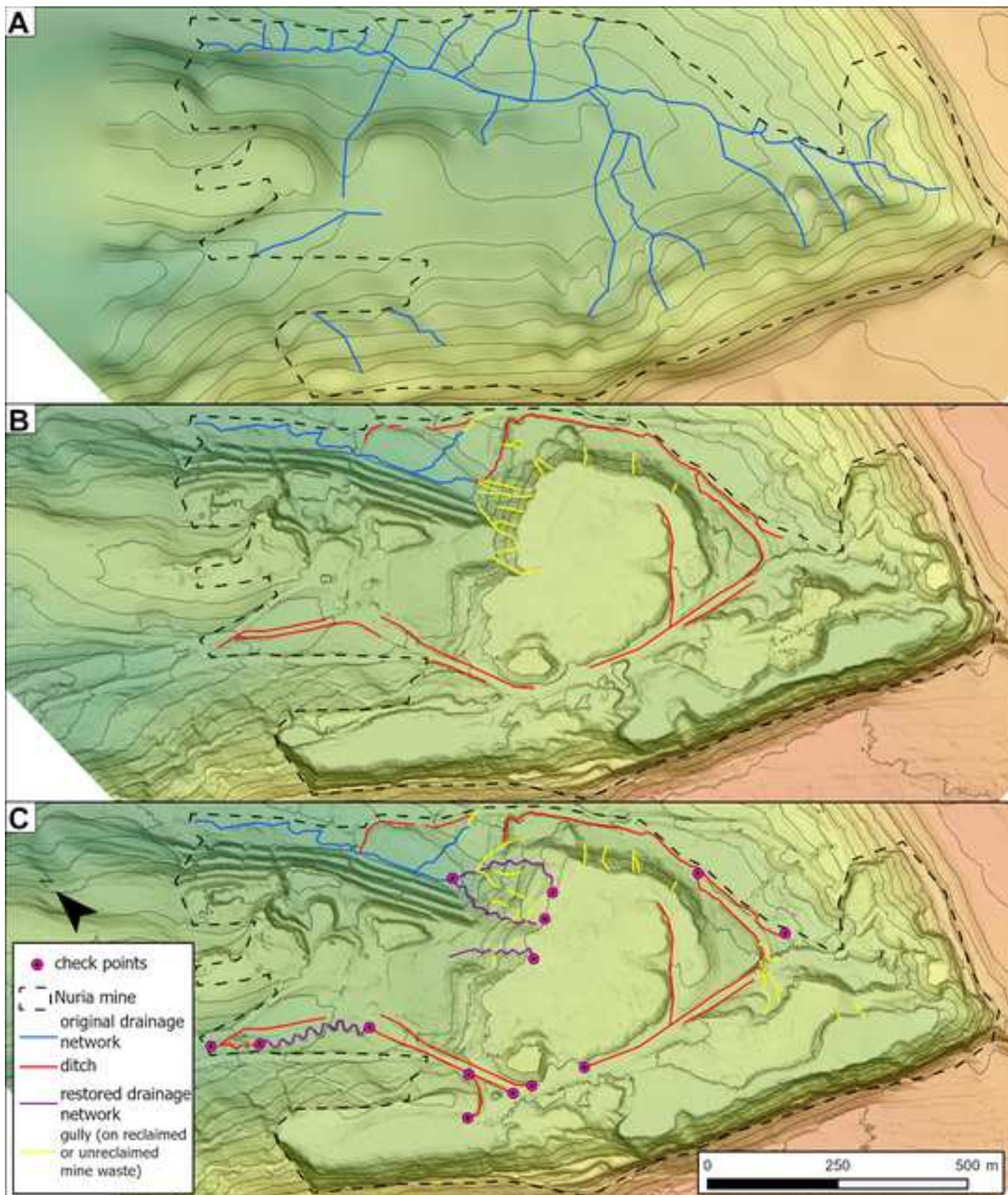


Figure 4

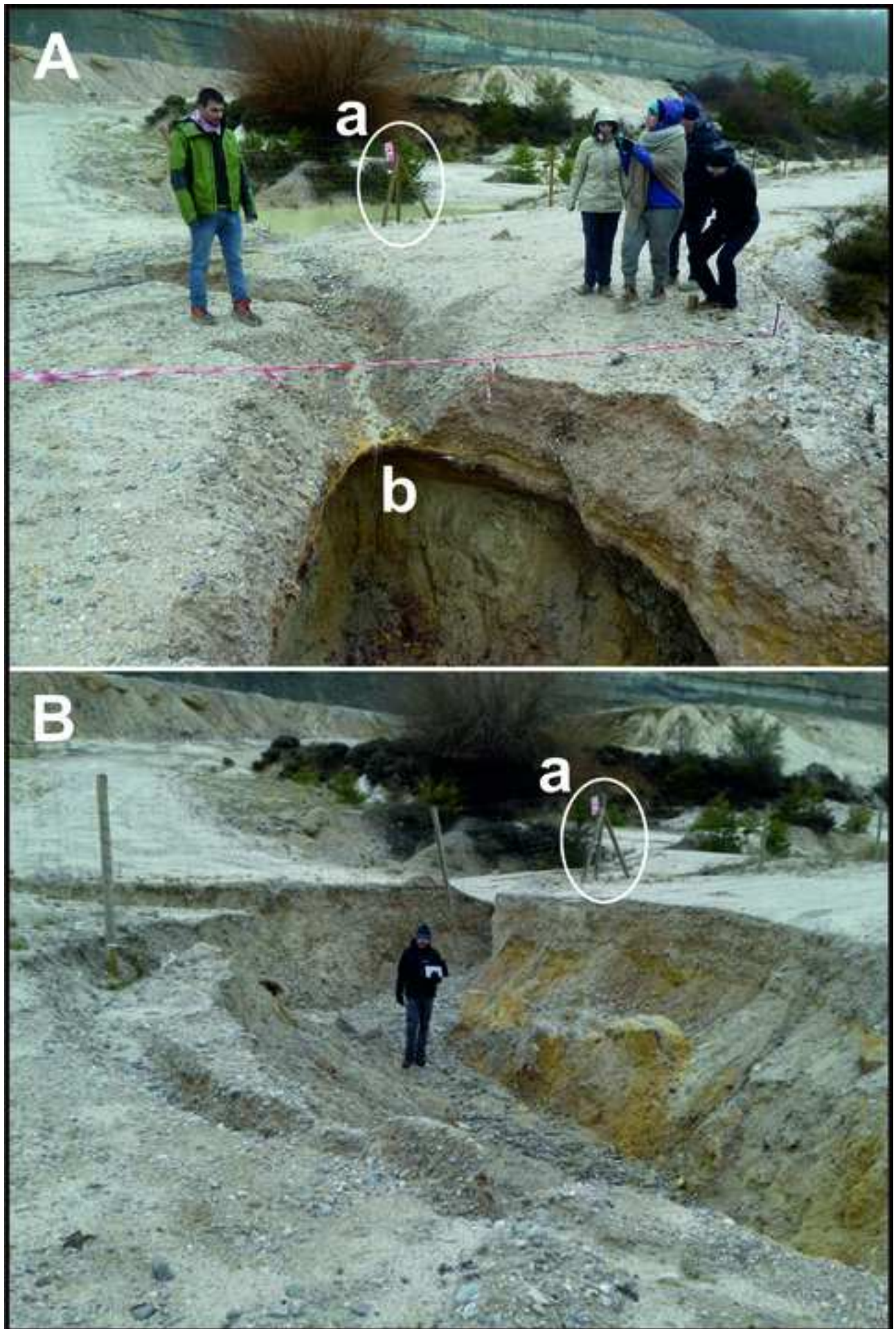


Figure 5

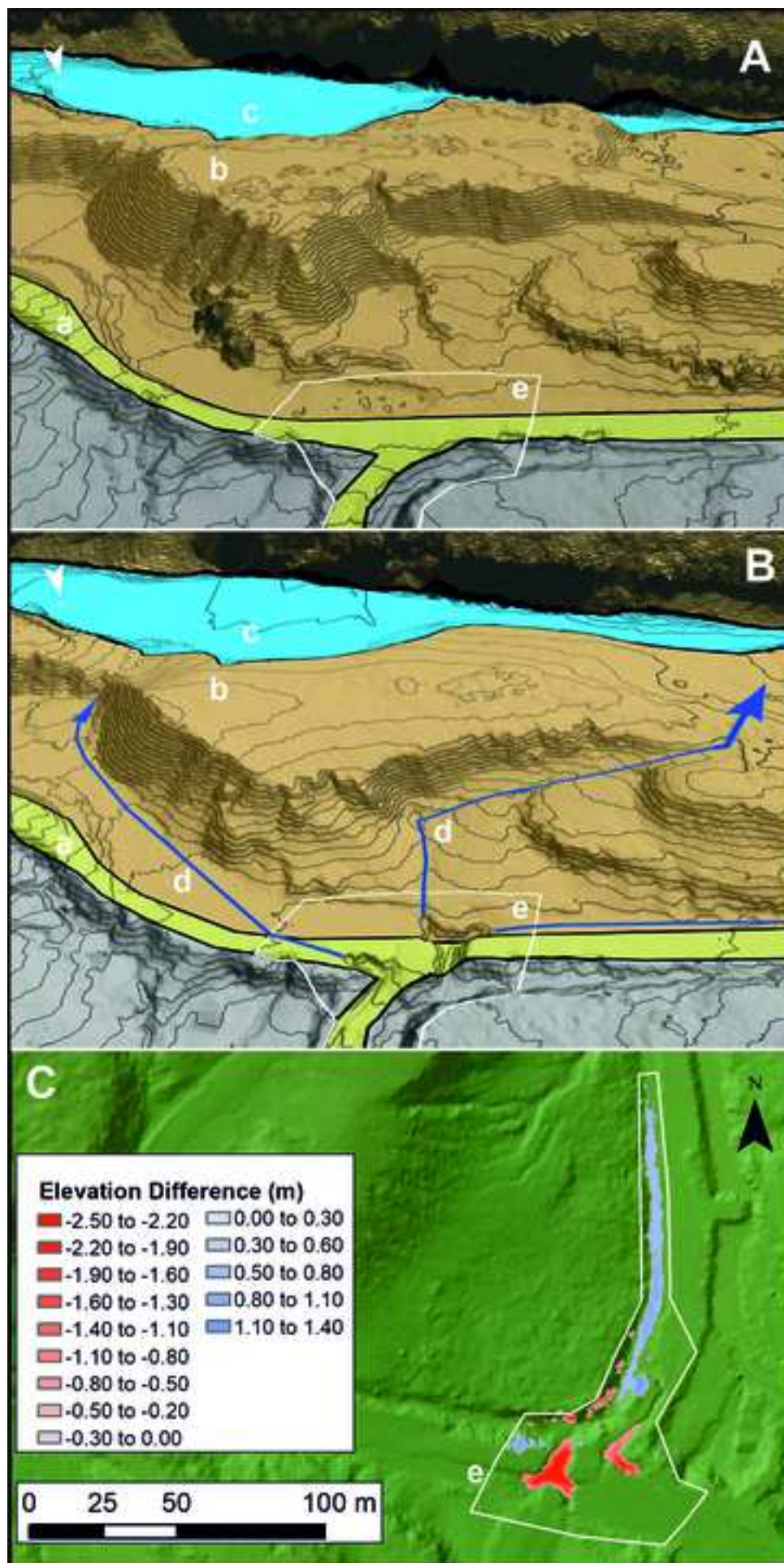


Figure 6

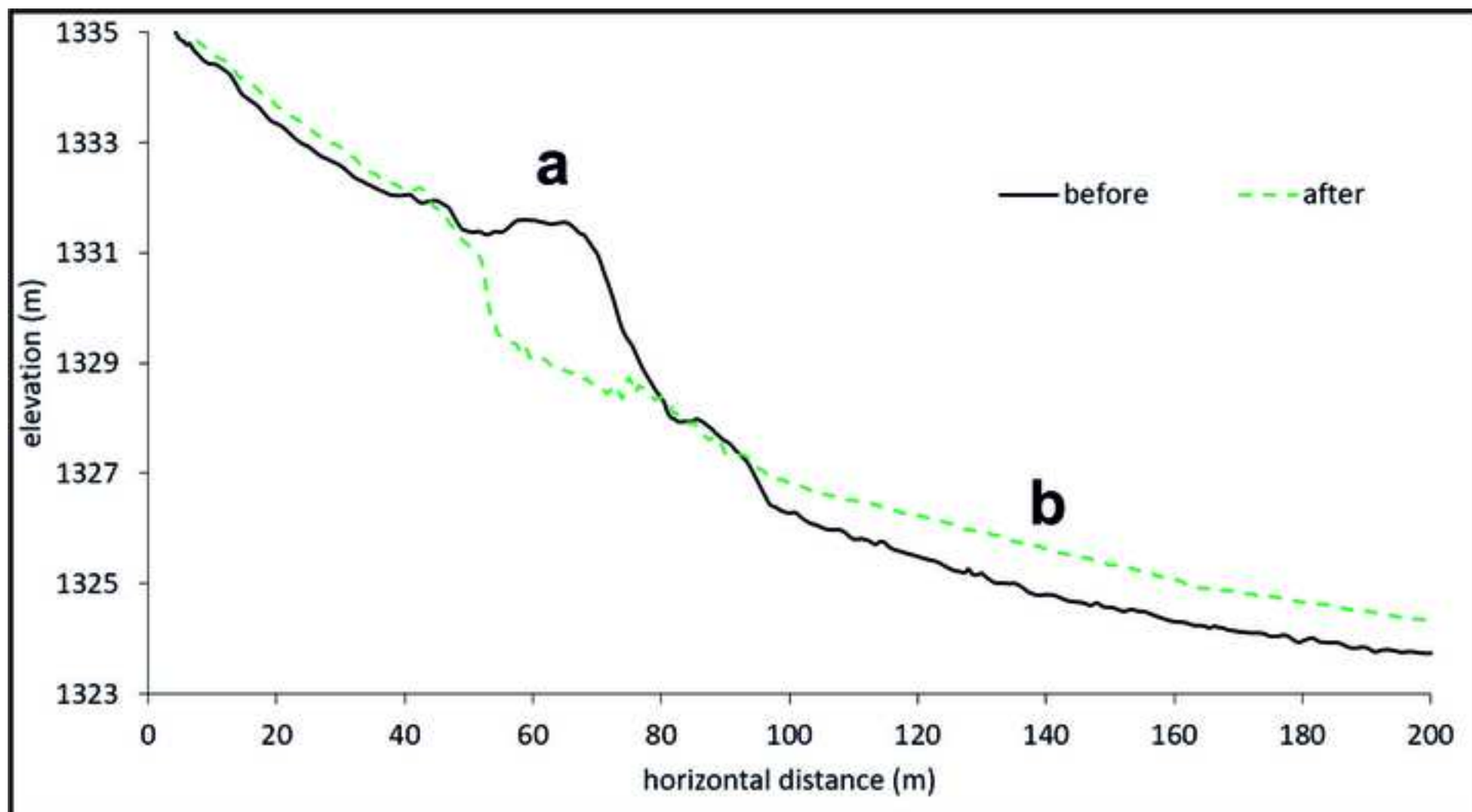


Figure 7



Figure 8

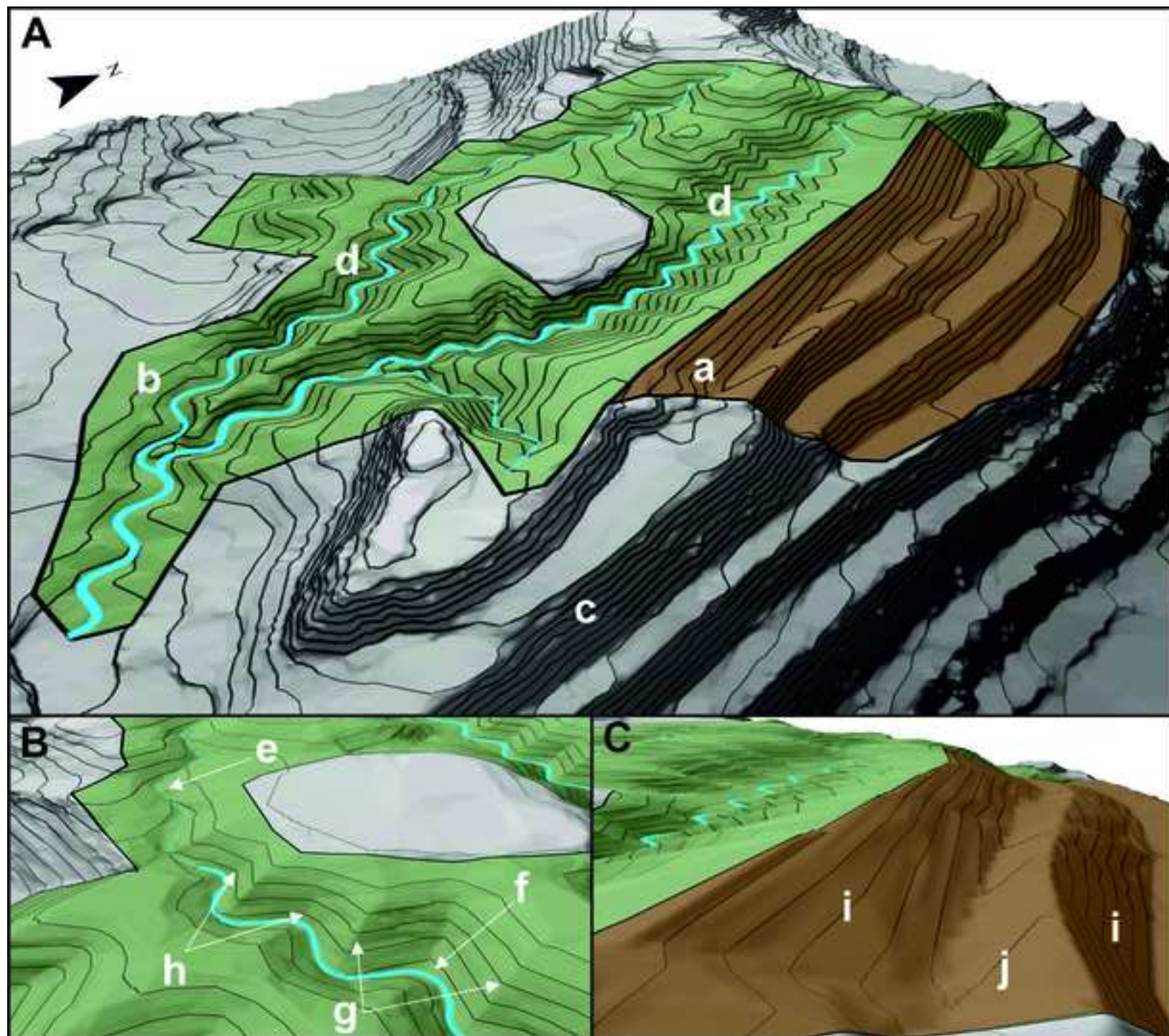


Figure 9

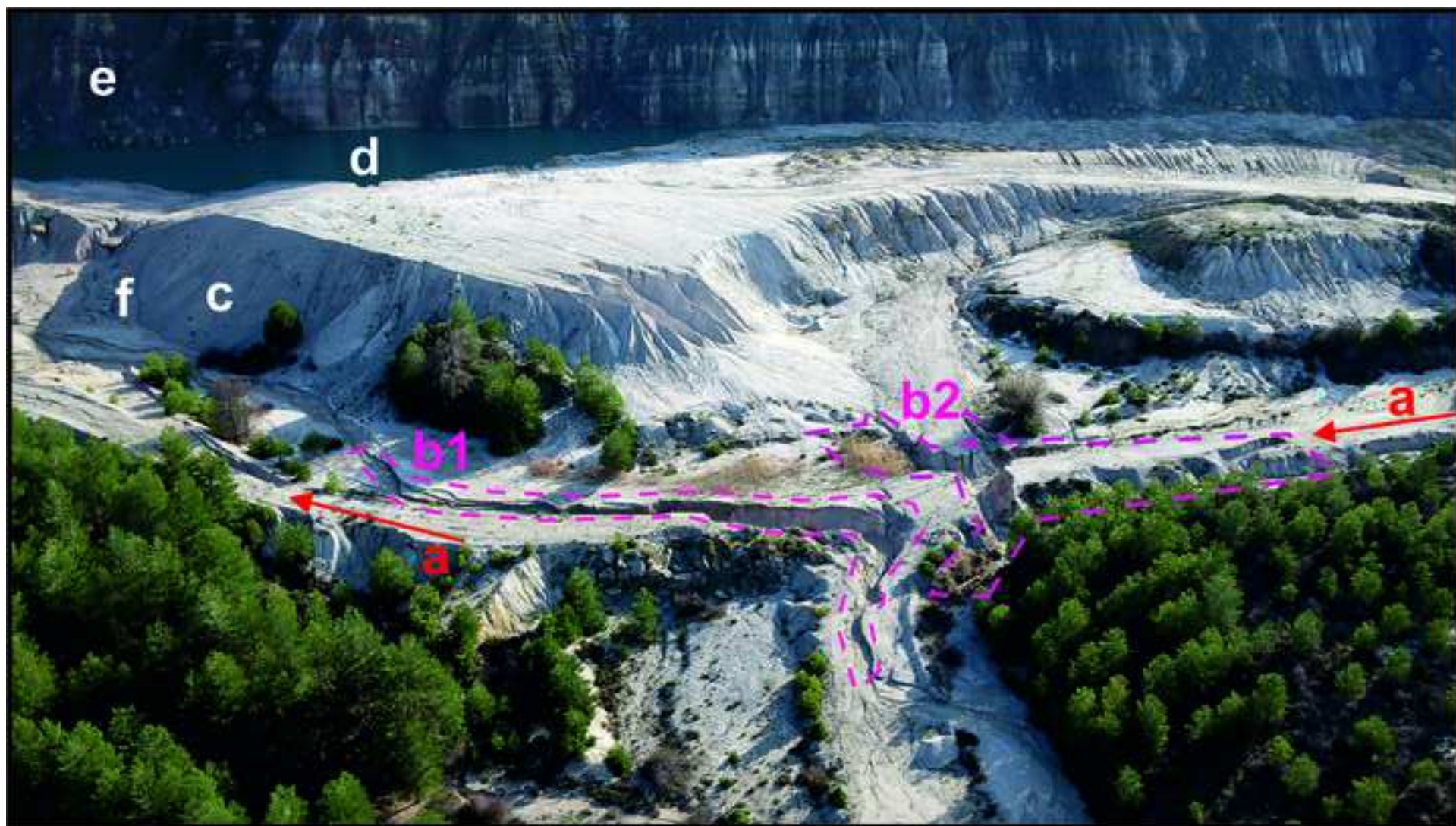
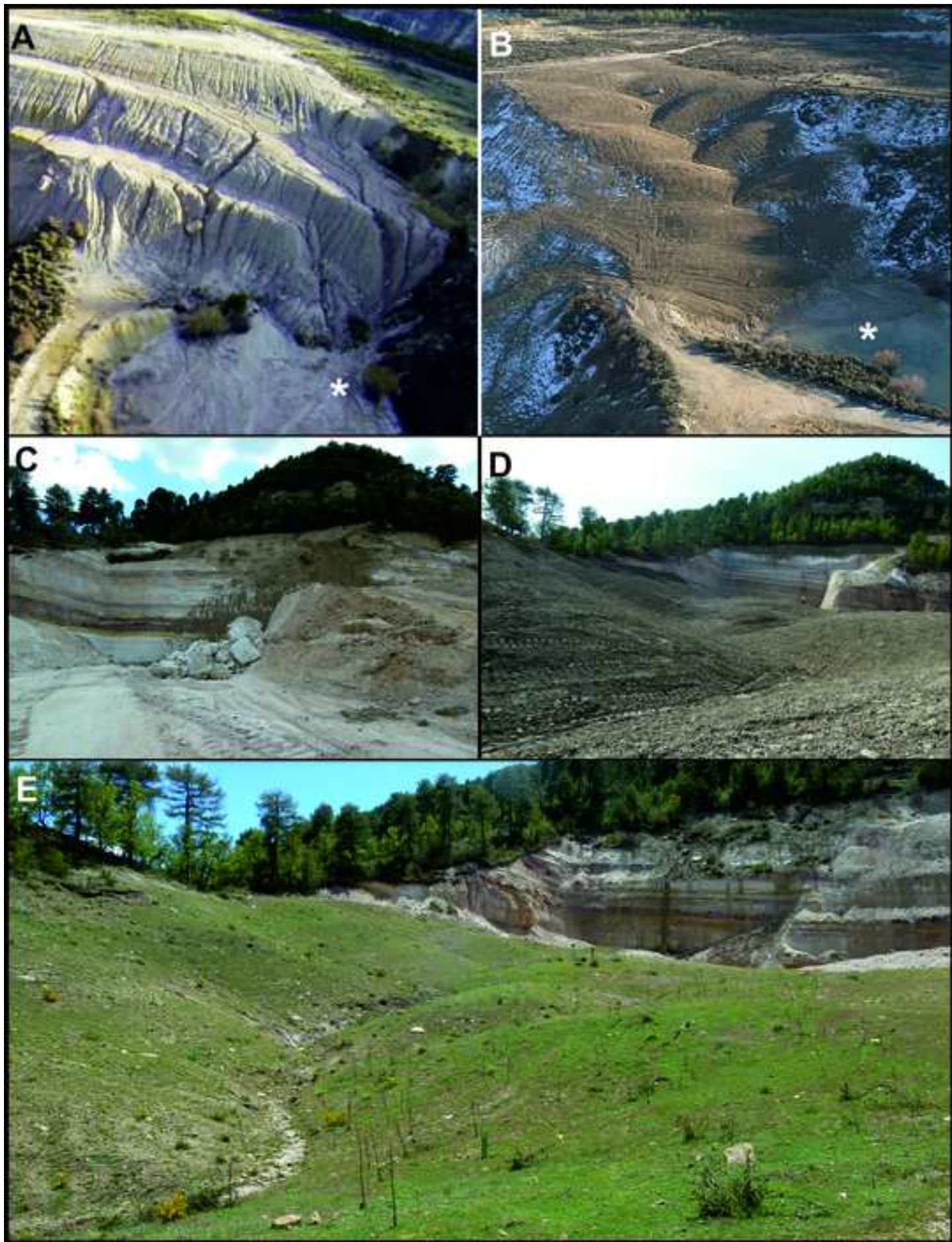


Figure 10



Declaration of interests

The authors declare that they have no known competing financial interests or personal relationships that could have appeared to influence the work reported in this paper.

The authors declare the following financial interests/personal relationships which may be considered as potential competing interests: